

## Electronic Supplementary Information

# *N*- and *S*-donor leaving groups in triazole-based ruthena(II)cycles: Potent anticancer activity, selective activation, and mode of action studies

Christoph A. Riedl<sup>a,b</sup>, Michaela Hejl<sup>a</sup>, Matthias H.M. Klose<sup>a,b</sup>, Alexander Roller<sup>a</sup>, Michael A. Jakupec<sup>a,b</sup>,  
Wolfgang Kandioller<sup>a,b\*</sup>, and Bernhard K. Keppler<sup>a,b</sup>

(a) Institute of Inorganic Chemistry, Faculty of Chemistry, University of Vienna, and (b) Research Cluster  
“Translational Cancer Therapy Research”, Waehringer Str. 42, 1090 Vienna, Austria

(\*) wolfgang.kandioller@univie.ac.at, Tel: +43-1-4277-52609; Fax: +43-1-4277-9526

### Table of Contents

1.	Experimental and calculated pKa values .....	2
2.	NMR investigations .....	3
3.	Single crystal x-ray diffraction analysis .....	5
4.	Stability in aqueous solution .....	14
5.	Oxidation of <b>3a</b> .....	18
6.	Amino acid binding studies .....	19
7.	Chromatographic lipophilicity index $\phi_0$ .....	23
8.	ROS generation .....	24
9.	Methyl green DNA intercalation assay .....	26
10.	Flow cytometric detection of apoptotic cells .....	27
11.	$^1\text{H}$ and $^{13}\text{C}$ NMR spectra .....	28

## 1. Experimental and calculated pKa values

**Table S1** Experimentally measured and calculated (ACD/Labs) pK<sub>a</sub> values (conjugated acid) of the metal-coordinating nitrogen donor atom at 25 °C.

Respective Complex	Ligand	pK <sub>a</sub>	Reference	calculated pK <sub>a</sub> <sup>b</sup>
<b>2a</b>	1 <i>H</i> -Imidazole	6.99	CRC Handbook <sup>3</sup>	7.18 ± 0.61
<b>2b</b>	1-Methylimidazole	6.95	CRC Handbook <sup>3</sup>	7.01 ± 0.10
<b>2c</b>	4-Phenylimidazole	-	-	6.68 ± 0.10
<b>2d</b>	1 <i>H</i> -Pyrazole	2.49	CRC Handbook <sup>3</sup>	2.83 ± 0.10
<b>2e</b>	1 <i>H</i> -Indazole	1.31 <sup>a</sup>	Catalán et al. <sup>4</sup>	1.26 ± 0.10
<b>2f</b>	Pyridine	5.23	CRC Handbook <sup>3</sup>	5.23 ± 0.10
<b>2g</b>	Isoquinoline	5.4	CRC Handbook <sup>3</sup>	5.37 ± 0.23
<b>2h</b>	Imidazo[1,2-a]pyridine	6.79 <sup>a</sup>	Catalán et al. <sup>4</sup>	6.80 ± 0.30
<b>2i</b>	Benzothiazole	1.2	Eicher et al. <sup>5</sup>	0.85 ± 0.10

a) Corrected to 25 °C

b) Calculated using Advanced Chemistry Development (ACD/Labs) Software V11.02 (© 1994-2017 ACD/Labs)

## 2. NMR investigations

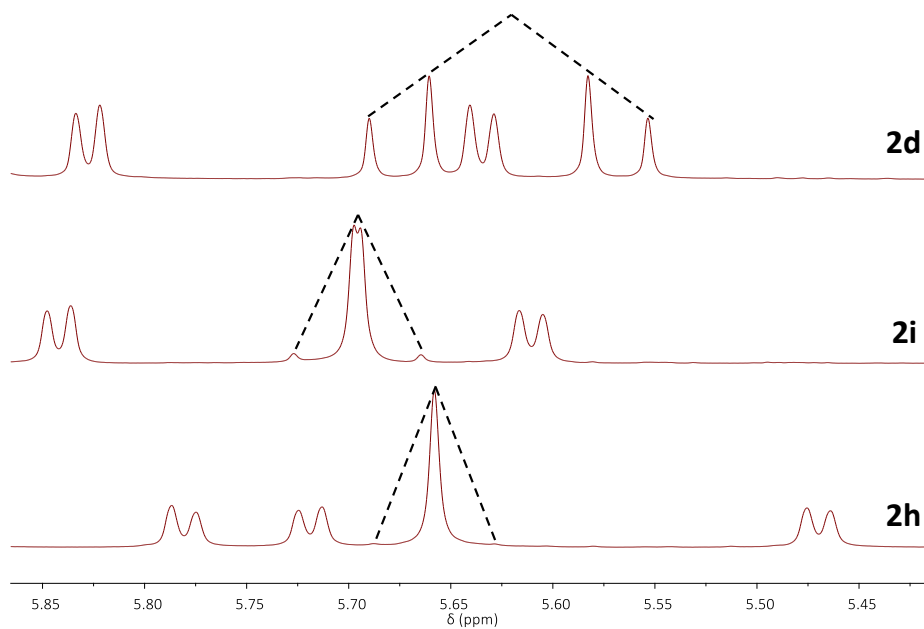


**Figure S1**  $^1\text{H}$  NMR spectra of **2d** (top), **2i** (middle), and **2h** (bottom) with dashed lines highlighting roof effect.

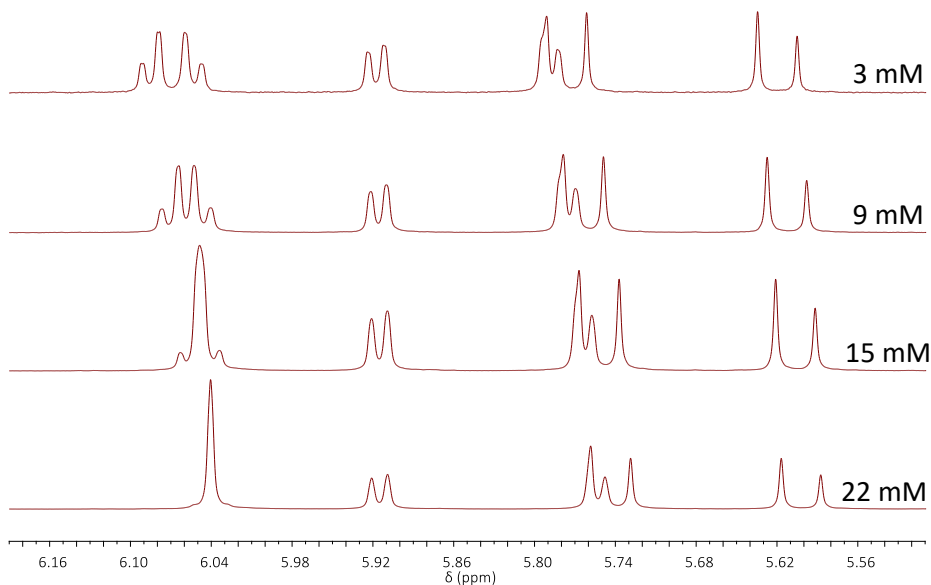


**Figure S2**  $^1\text{H}$  NMR of **2e** at four different concentrations in  $\text{CDCl}_3$ , illustrating the concentration-dependence of aromatic arene and methylene protons.

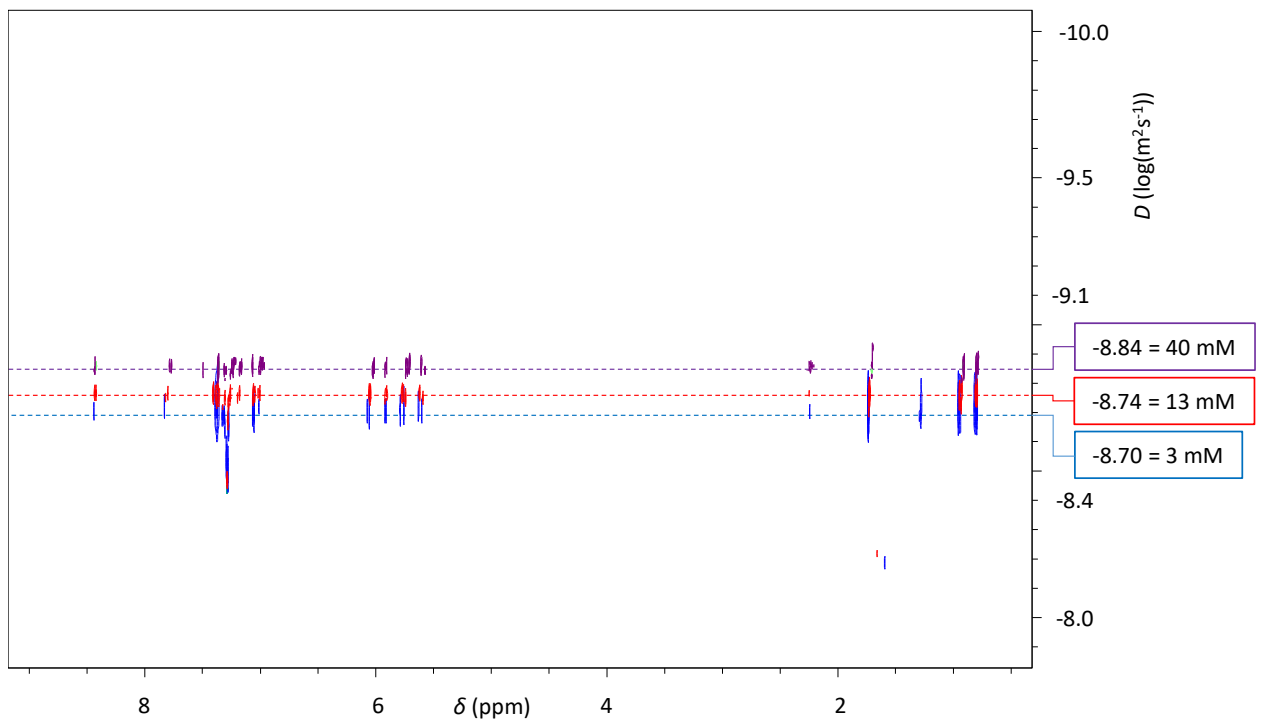


**Figure S3** Overlay of <sup>1</sup>H DOSY NMR spectra of **2e** recorded at three different concentrations in  $\text{CDCl}_3$ .

### 3. Single crystal x-ray diffraction analysis

**Table S2** Experimental parameters and CCDC codes.

Sample	Diffracto-meter	Source	Temp. [K]	Detector distance [mm]	Time per frame [s]	No. of frames	Frame width [°]	CCDC
<b>2e</b>	X8	Mo	100	35	50	2835	0.5	1575667
<b>2i</b>	X8	Mo	100	35	30	1773	0.5	1575668
<b>3a</b>	D8	Mo	100	34	24	1419	0.5	1575669

**Table S3** Selected bond lengths.

Compound	Bond lengths (Å)								
	Ru-LG	Ru-N3	Ru-PhC2	PhC1-PhC2	PhC2-PhC3	PhC3-PhC4	PhC4-PhC5	PhC5-PhC6	PhC6-PhC1
<b>1<sub>A</sub></b>	2.4280(18)	2.069(6)	2.057(6)	1.429(9)	1.431(9)	1.387(9)	1.394(10)	1.401(10)	1.383(9)
<b>1<sub>B</sub></b>	2.4165(17)	2.067(6)	2.063(6)	1.418(9)	1.416(9)	1.365(8)	1.410(10)	1.383(9)	1.398(9)
<b>2e<sub>A</sub></b>	2.087(4)	2.058(4)	2.077(5)	1.413(8)	1.385(8)	1.408(9)	1.372(11)	1.377(10)	1.394(8)
<b>2e<sub>B</sub></b>	2.088(4)	2.067(4)	2.082(5)	1.398(8)	1.397(7)	1.385(8)	1.376(9)	1.376(9)	1.392(8)
<b>2i<sub>A</sub></b>	2.130(3)	2.068(3)	2.072(4)	1.415(5)	1.401(6)	1.399(6)	1.380(6)	1.392(6)	1.393(5)
<b>2i<sub>B</sub></b>	2.110(3)	2.086(3)	2.083(4)	1.408(6)	1.397(5)	1.401(5)	1.384(6)	1.388(5)	1.390(5)
<b>3a</b>	2.3620(4)	2.0607(13)	2.0761(17)	1.419(2)	1.400(2)	1.396(3)	1.386(4)	1.391(3)	1.393(3)

**Table S4** Selected bond lengths.

Compound	Bond lengths (Å)							
	N1–N2	N2–N3	N3–C4	C4–C5	C5–N1	C4–PhC1	N1–BnCH <sub>2</sub>	Ring slippage <sup>a</sup>
<b>1<sub>A</sub></b>	1.338(7)	1.329(8)	1.367(8)	1.372(10)	1.365(8)	1.451(10)	1.451(8)	0.095
<b>1<sub>B</sub></b>	1.351(7)	1.324(7)	1.368(8)	1.382(9)	1.345(8)	1.472(9)	1.470(8)	0.095
<b>2e<sub>A</sub></b>	1.341(7)	1.309(6)	1.376(7)	1.386(8)	1.334(9)	1.441(8)	1.464(7)	0.082
<b>2e<sub>B</sub></b>	1.324(7)	1.318(6)	1.360(7)	1.368(8)	1.345(8)	1.458(7)	1.480(7)	0.077
<b>2i<sub>A</sub></b>	1.339(5)	1.327(4)	1.361(5)	1.379(5)	1.347(5)	1.455(5)	1.480(5)	0.082
<b>2i<sub>B</sub></b>	1.346(4)	1.320(4)	1.369(5)	1.369(5)	1.351(5)	1.456(5)	1.462(5)	0.077
<b>3a</b>	1.342(2)	1.3214(19)	1.366(2)	1.377(2)	1.348(2)	1.450(2)	1.468(2)	0.064

(a) Distance between the perpendicular projection of an heavy atom on the ring l.s.-plane and the arene ring

**Table S5** Selected bond angles.

Compound	Bond angles [°]								
	PhC2–Ru–LG	LG–Ru–N3	N3–Ru–PhC2	Ru–PhC2–PhC1	Ru–PhC2–PhC3	PhC1–C4–C5	PhC1–C4–N3	Ru–N3–N2	Ru–N3–C4
<b>1<sub>A</sub></b>	87.29(17)	84.99(15)	77.4(3)	117.4(5)	128.1(5)	138.5(6)	115.5(6)	130.4(4)	117.5(5)
<b>1<sub>B</sub></b>	86.95(16)	86.58(14)	77.5(2)	117.0(5)	115.0(6)	138.9(6)	114.0(6)	131.4(4)	118.3(4)
<b>2e<sub>A</sub></b>	84.53(19)	86.19(17)	77.7(2)	116.1(4)	126.6(4)	139.6(6)	115.1(5)	131.1(4)	117.4(4)
<b>2e<sub>B</sub></b>	85.01(18)	87.77(17)	77.30(18)	116.1(4)	127.3(4)	138.9(5)	114.5(5)	130.8(4)	117.9(3)
<b>2i<sub>A</sub></b>	85.67(13)	90.75(12)	77.24(15)	116.6(3)	127.1(3)	138.5(4)	114.6(3)	130.2(3)	118.1(3)
<b>2i<sub>B</sub></b>	87.26(13)	88.58(12)	77.22(13)	116.5(3)	127.0(3)	138.2(4)	114.8(3)	131.5(2)	117.5(2)
<b>3a</b>	86.90(5)	89.73(4)	77.52(6)	116.17(12)	127.52(14)	138.33(17)	115.01(14)	130.81(11)	117.90(11)

**Table S6** Selected torsion angles.

Compound	Torsion angles [°]		
	BnCH <sub>2</sub> –N1–C5–C4	N3–C4–PhC1–PhC2	C5–N1–BnCH <sub>2</sub> –BnC1
<b>1<sub>A</sub></b>	177.2(5)	-4.4(8)	82.7(8)
<b>1<sub>B</sub></b>	-179.7(5)	-2.9(7)	90.4(7)
<b>2e<sub>A</sub></b>	-169.6(5)	0.4(7)	83.4(8)
<b>2e<sub>B</sub></b>	168.4(5)	-1.4(6)	-83.9(7)
<b>2i<sub>A</sub></b>	-176.8(3)	-2.7(4)	94.4(5)
<b>2i<sub>B</sub></b>	-179.9(3)	-3.0(5)	-90.9(5)
<b>3a</b>	174.10(16)	-0.5(2)	-71.6(2)

3.1.  $[(2-\kappa N)-1H\text{-Indazole})(1\text{-benzyl-}4-(2'\text{-}\kappa C)\text{-phenyl-}1,2,3\text{-(3-}\kappa N\text{)}\text{-triazolato})(\eta^6\text{-}p\text{-cymene})\text{ruthenium(II)] nitrate}$  (**2e**)

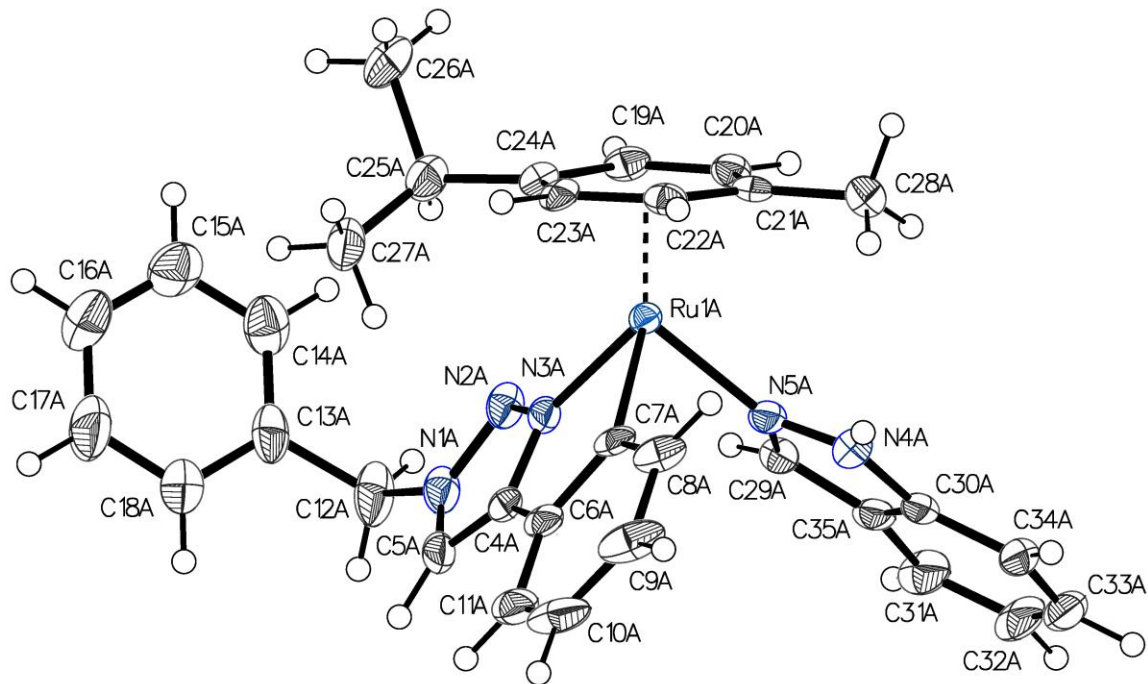


**Figure S4** Crystal structure of **2e**, drawn with 50% displacement ellipsoids. The second molecule of the asymmetric unit, solvent molecules and counter ions were omitted for clarity.

**Table S7** Sample and crystal data of **2e**.

Chemical formula	$C_{64}H_{66}N_{12}O_7Ru_2$	
Formula weight (g/mol)	1317.42	
Temperature (K)	100	
Measurement method	\f and \w scans	
Radiation wavelength (Å)	MoKα ( $\lambda = 0.71073$ )	
Crystal size (mm <sup>3</sup> )	$0.23 \times 0.06 \times 0.025$	
Crystal habit		
Density (calculated) (g/cm <sup>3</sup> )	1.422	
Abs. correction T <sub>min</sub>	0.6739	
Abs. correction type	multi-scan	
Crystal system	monoclinic	
Space group	$P2_1/c$	
Z	4	
Volume (Å <sup>3</sup> )	6151.8(11)	
Unit cell dimensions (Å) and (°)	10.6875(11)	90
	22.259(2)	90.648(4)
	25.861(3)	90
Absorption coefficient (mm <sup>-1</sup> )	0.554	
Abs. correction T <sub>max</sub>	0.7460	
F(000) (e <sup>-</sup> )	2712	

**Table S8** Data collection and structure refinement parameters of **2e**.

Index ranges	-12 ≤ h ≤ 12, -25 ≤ k ≤ 26 -31 ≤ l ≤ 31	Theta range for data collection (°)	3.642 to 50.7				
Reflections number	166872	Data / restraints / parameters	11203 / 165 / 764				
Refinement method	Least squares	Final R indices	<table border="1"> <tr> <td>all data</td> <td><math>R_1 = 0.0791</math> <math>wR_2 = 0.1627</math></td> </tr> <tr> <td><math> &gt;2\sigma(I) </math></td> <td><math>R_1 = 0.0563</math> <math>wR_2 = 0.1492</math></td> </tr> </table>	all data	$R_1 = 0.0791$ $wR_2 = 0.1627$	$ >2\sigma(I) $	$R_1 = 0.0563$ $wR_2 = 0.1492$
all data	$R_1 = 0.0791$ $wR_2 = 0.1627$						
$ >2\sigma(I) $	$R_1 = 0.0563$ $wR_2 = 0.1492$						
Function minimized	$\Sigma w(Fo^2 - Fc^2)^2$	Weighting scheme	$w=1/[s^2 (Fo^2)+(0.0717P)^2 +33.9060P]$ where $P=(Fo^2+2Fc^2)/3$				
Goodness-of-fit on $F^2$	1.042						
Largest diff. peak and hole [ $e \text{ \AA}^{-3}$ ]	2.06/-2.01						

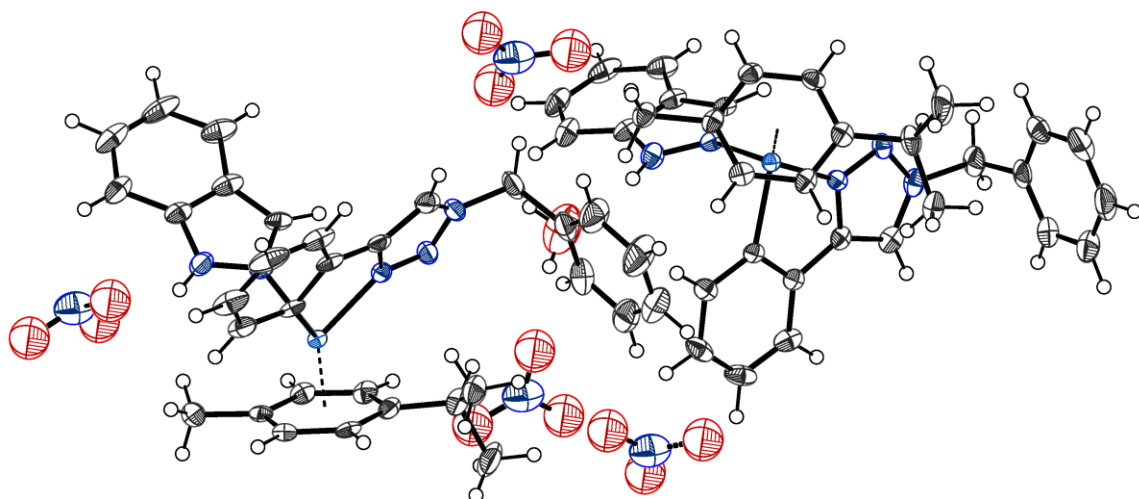


**Figure S5** Asymmetric unit of **2e**, drawn with 50% displacement ellipsoids. Four  $\text{NO}_3^-$  must be part of the asymmetric unit as evidenced by other analyses presented herein. Four positions could be characterized, but we believe that there is a fifth position to part for  $\text{NO}_3^-$  as visualized by the displacement ellipsoids and confirmed by the need to cut solvent-available void. Details about the excluded volume are part of the cif (`_refine_special_details & _shelx_fab_file`).

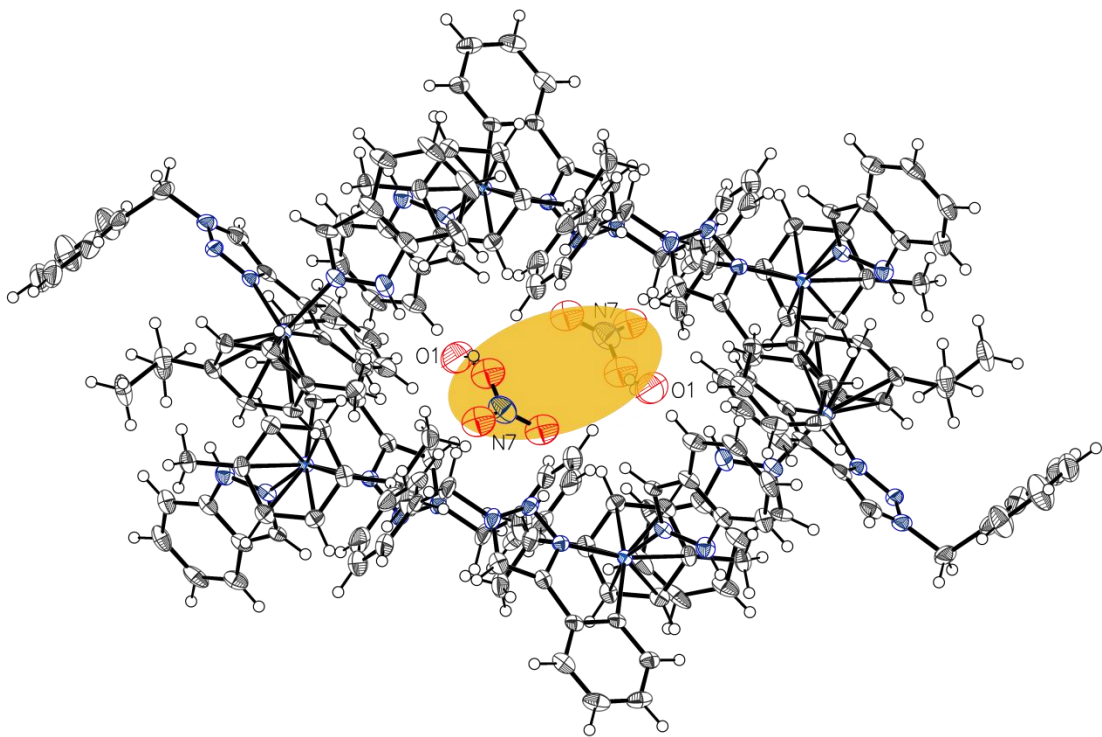


**Figure S6** It was not possible to locate approximately 53% of one of two disordered  $\text{NO}_3^-$  ions in the unit cell. The orange ellipsoid describes the location of the corresponding  $\text{NO}_3^-$  accessible void. The HKL masked volume is two times  $191.2 \text{ \AA}^3$  per unit cell, and the electron content is two times 45.8 per unit cell. This indicates that in addition to the missing nitrate, also some water molecules are present in the available void.  $\text{NO}_3^-$  was fixed with the help of DFIX and EADP.

3.2.  $[(\kappa\text{N}-1,3\text{-Benzothiazole})(1\text{-benzyl-}4\text{-(2'-}\kappa\text{C)\text{-phenyl-}1,2,3\text{-(3-}\kappa\text{N)\text{-triazolato})(}\eta^6\text{-}p\text{-cymene)ruthenium(II)] nitrate (2i)}$

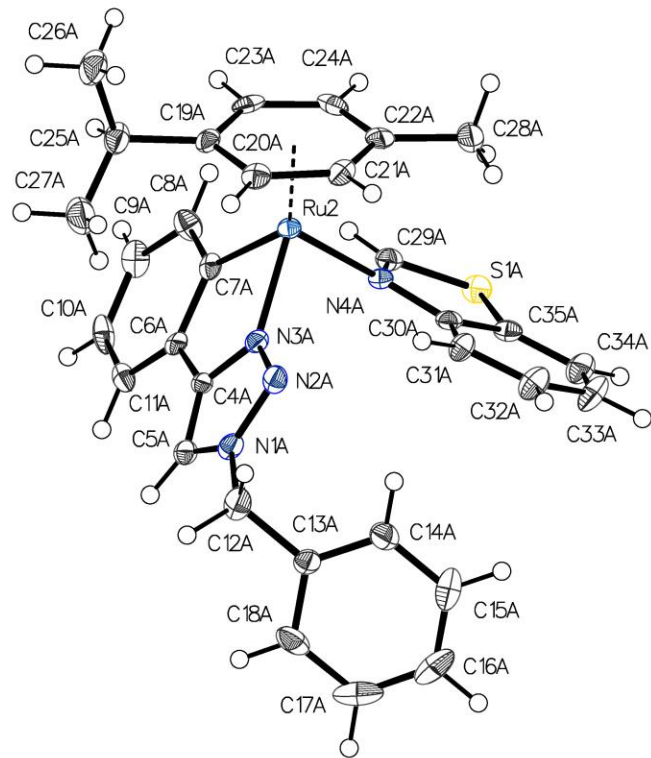


**Figure S7** Crystal structure of **2i**, drawn with 50% displacement ellipsoids. The second molecule of the asymmetric unit, solvent molecules and counter ions were omitted for clarity.

**Table S9** Sample and crystal data of **2i**.

Chemical formula	$\text{C}_{33}\text{H}_{34}\text{Cl}_2\text{N}_5\text{O}_{3.5}\text{RuS}$	
Formula weight (g/mol)	760.68	
Temperature (K)	100	
Measurement method	\f and \w scans	
Radiation wavelength (Å)	MoK $\alpha$ ( $\lambda = 0.71073$ )	
Crystal size (mm <sup>3</sup> )	0.12 × 0.08 × 0.03	
Crystal habit	Clear yellow needle	
Density (calculated) (g/cm <sup>3</sup> )	1.538	
Abs. correction T <sub>min</sub>	0.6935	
Abs. correction type	multi-scan	
Crystal system	triclinic	
Space group	P-1	
Z	4	
Volume (Å <sup>3</sup> )	3284.4(4)	
Unit cell dimensions (Å) and (°)	12.0373(8)	95.649(2)
	13.4469(8)	95.099(3)
	20.7463(15)	98.748(2)
Absorption coefficient (mm <sup>-1</sup> )	0.748	
Abs. correction T <sub>max</sub>	0.7460	
F(000) (e <sup>-</sup> )	1556	

**Table S10** Data collection and structure refinement parameters of **2i**.

Index ranges	-14 ≤ h ≤ 14 -11 ≤ k ≤ 16 -24 ≤ l ≤ 24	Theta range for data collection (°)	3.968 to 50.698				
Reflections number	57798	Data / restraints / parameters	11970 / 21 / 845				
Refinement method	Least squares	Final R indices	<table border="1"> <tr> <td>all data</td> <td><math>R_1 = 0.0666</math> <math>wR_2 = 0.1197</math></td> </tr> <tr> <td><math> I  &gt; 2\sigma(I)</math></td> <td><math>R_1 = 0.0469</math> <math>wR_2 = 0.1100</math></td> </tr> </table>	all data	$R_1 = 0.0666$ $wR_2 = 0.1197$	$ I  > 2\sigma(I)$	$R_1 = 0.0469$ $wR_2 = 0.1100$
all data	$R_1 = 0.0666$ $wR_2 = 0.1197$						
$ I  > 2\sigma(I)$	$R_1 = 0.0469$ $wR_2 = 0.1100$						
Function minimized	$\Sigma w(F_o^2 - F_c^2)^2$	Weighting scheme	$w = 1/[s^2 (F_o^2) + (0.0596P)^2]$ where $P = (F_o^2 + 2F_c^2)/3$				
Goodness-of-fit on $F^2$	0.981						
Largest diff. peak and hole [ $e \text{ \AA}^{-3}$ ]	1.21 / -1.38						

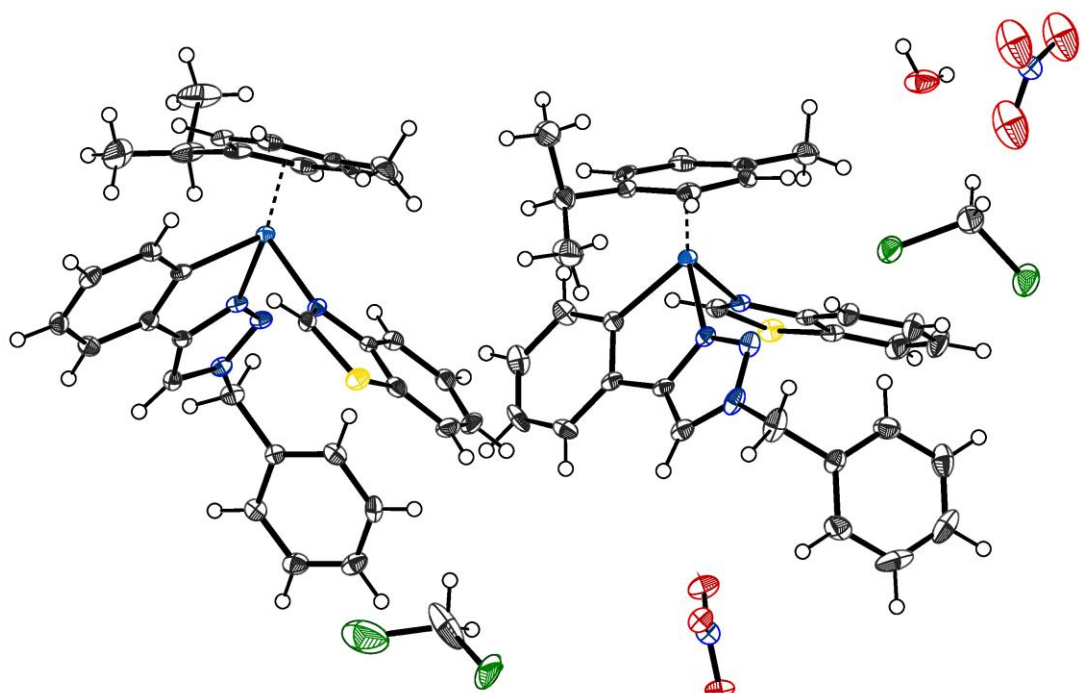


**Figure S8** Asymmetric unit of **2i**, drawn with 50% displacement ellipsoids. Disordered solution (DCM) was omitted for clarity.

3.3. [( $\kappa$ S-(Methylsulfanyl)methane)(1-benzyl-4-(2'- $\kappa$ C)-phenyl-1,2,3-(3- $\kappa$ N)-triazolato]( $\eta^6$ -*p*-cymene)ruthenium(II)] nitrate (**3a**)

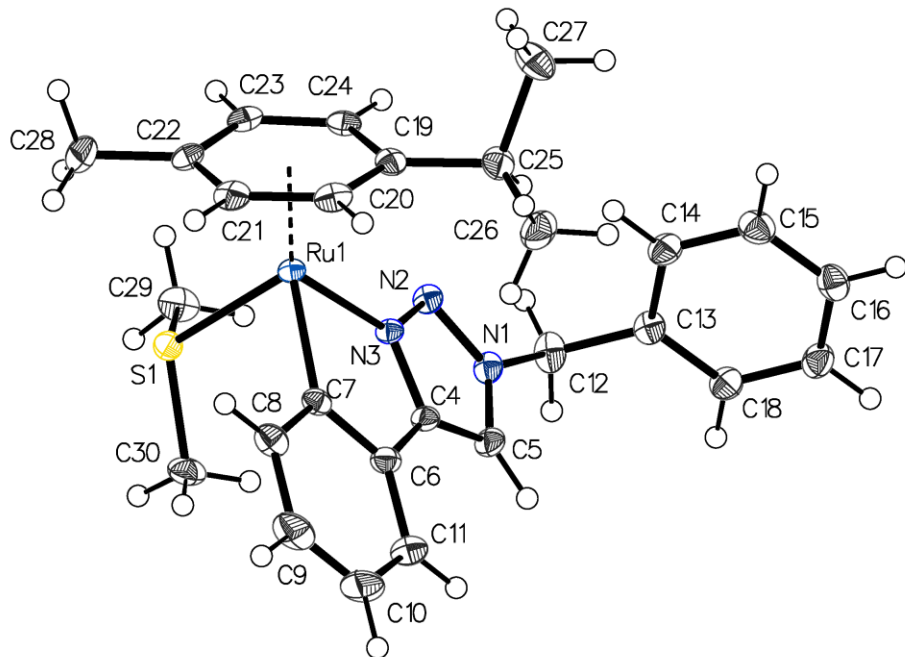


**Figure S9** Crystal structure of **3a**, drawn with 50% displacement ellipsoids, the counterion is omitted for clarity.

**Table S11** Sample and crystal data of **2e**.

Chemical formula	$C_{27}H_{32}N_4O_3RuS$	
Formula weight (g/mol)	593.69	
Temperature (K)	100	
Measurement method	\f and \w scans	
Radiation wavelength (Å)	MoK $\alpha$ ( $\lambda = 0.71073$ )	
Crystal size (mm <sup>3</sup> )	0.12 × 0.08 × 0.03	
Crystal habit	Clear yellow block	
Density (calculated) (g/cm <sup>3</sup> )	1.381	
Abs. correction T <sub>min</sub>	0.6449	
Abs. correction type	multi-scan	
Crystal system	triclinic	
Space group	P-1	
Z	2	
Volume (Å <sup>3</sup> )	1427.31(14)	
Unit cell dimensions (Å) and (°)	9.8204(5)	98.178(2)
	11.5773(6)	107.253(2)
	15.0588(9)	113.792(2)
Absorption coefficient (mm <sup>-1</sup> )	0.656	
Abs. correction T <sub>max</sub>	0.7460	
F(000) (e <sup>-</sup> )	612	

**Table S12** Data collection and structure refinement parameters of **2e**.

Index ranges	-13 ≤ h ≤ 13 -16 ≤ k ≤ 16 -21 ≤ l ≤ 21	Theta range for data collection (°)	4.652 to 60.172				
Reflections number	39743	Data / restraints / parameters	8364 / 0 / 339				
Refinement method	Least squares	Final R indices	<table border="1"> <tr> <td>all data</td> <td><math>R_1 = 0.0338</math> <math>wR_2 = 0.0865</math></td> </tr> <tr> <td><math> I  &gt; 2\sigma(I)</math></td> <td><math>R_1 = 0.0319</math> <math>wR_2 = 0.0851</math></td> </tr> </table>	all data	$R_1 = 0.0338$ $wR_2 = 0.0865$	$ I  > 2\sigma(I)$	$R_1 = 0.0319$ $wR_2 = 0.0851$
all data	$R_1 = 0.0338$ $wR_2 = 0.0865$						
$ I  > 2\sigma(I)$	$R_1 = 0.0319$ $wR_2 = 0.0851$						
Function minimized	$\Sigma w(Fo^2 - Fc^2)^2$	Weighting scheme	$w=1/[s^2 (Fo^2)+(0.0482P)^2 +1.1984P]$ where $P=(Fo^2+2Fc^2)/3$				
Goodness-of-fit on $F^2$	1.09						
Largest diff. peak and hole [ $e \text{ \AA}^{-3}$ ]	1.61 / -1.48						

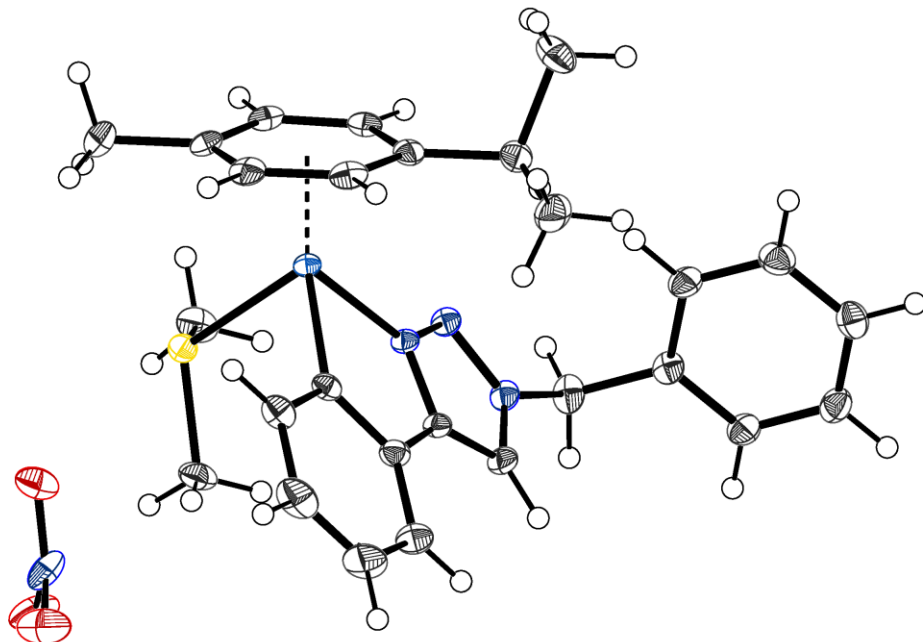


**Figure S10** Asymmetric unit of **3a**, drawn with 50% displacement ellipsoids. Disordered solution (nitrate) was omitted for clarity and solvent available void was cut. Details on the excluded volume can be found in the cif code (\_refine\_special\_details & \_shelx\_fab\_file)

#### 4. Stability in aqueous solution

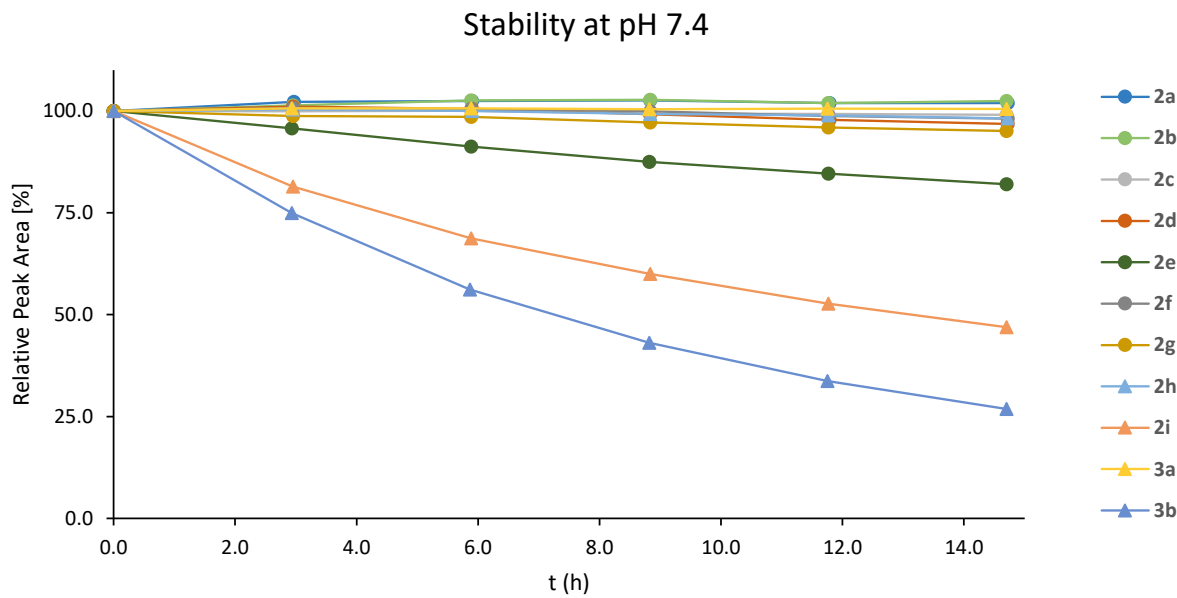


**Figure S11** Stability of complexes (50  $\mu$ M) in 1% DMF/phosphate buffer (40 mM, pH 7.4), expressed as relative decrease of the analyte peak area over time in uHPLC runs.

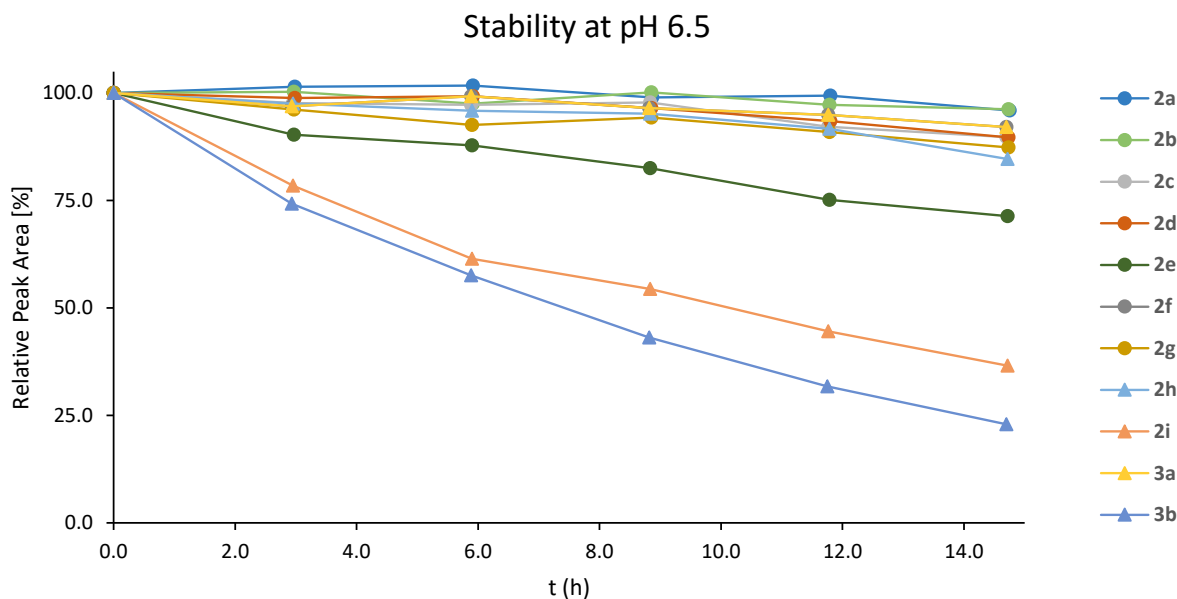


**Figure S12** Stability of complexes (50  $\mu$ M) in 1% DMF/phosphate buffer (40 mM, pH 6.5), expressed as relative decrease of the analyte peak area over time in uHPLC runs.

### Stability at pH 5.0

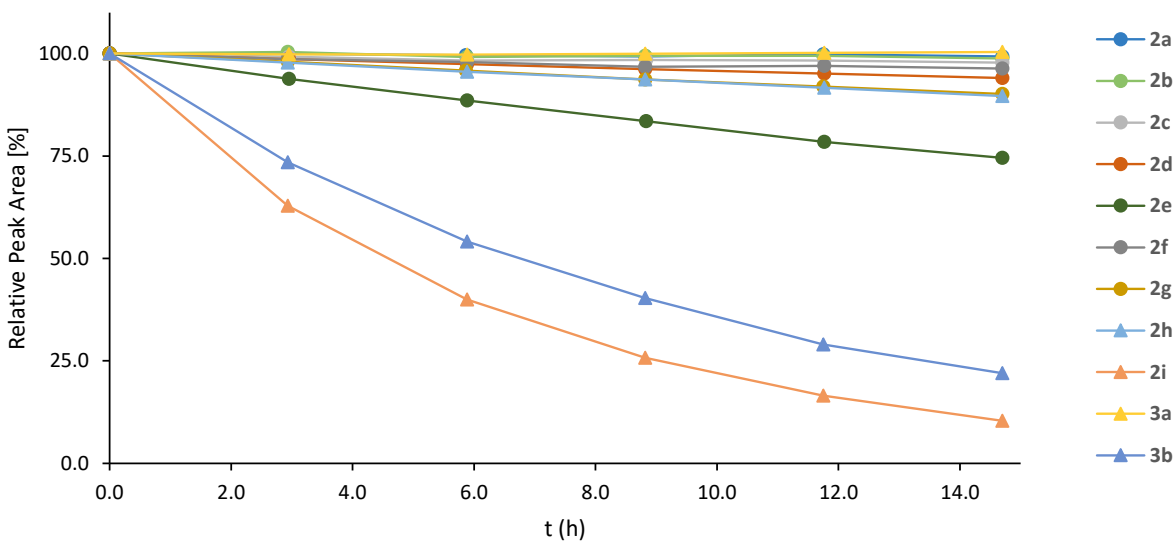


**Figure S13** Stability of complexes (50  $\mu$ M) in 1% DMF/ammonium acetate buffer (40 mM, pH 5.0), expressed as relative decrease of the analyte peak area over time in uHPLC runs.

### Stability at pH 3.0

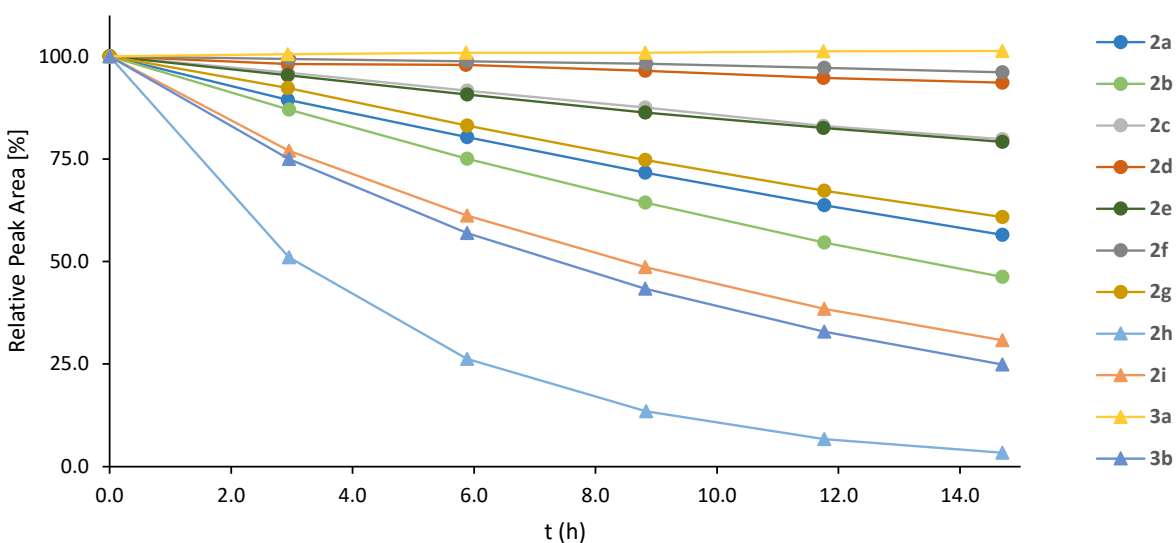


**Figure S14** Stability of complexes (50  $\mu$ M) in 1% DMF/phosphate buffer (40 mM, pH 3.0), expressed as relative decrease of the analyte peak area over time in uHPLC runs.

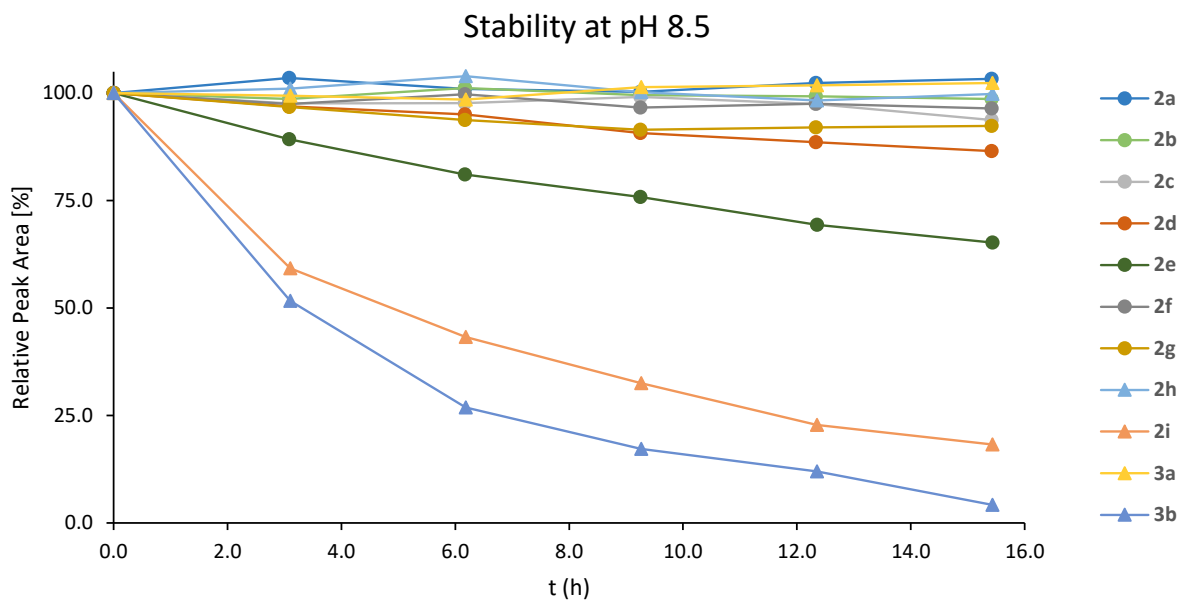


**Figure S15** Stability of complexes (50  $\mu\text{M}$ ) in 1% DMF/phosphate buffer (40 mM, pH 8.5), expressed as relative decrease of the analyte peak area over time in HPLC runs.

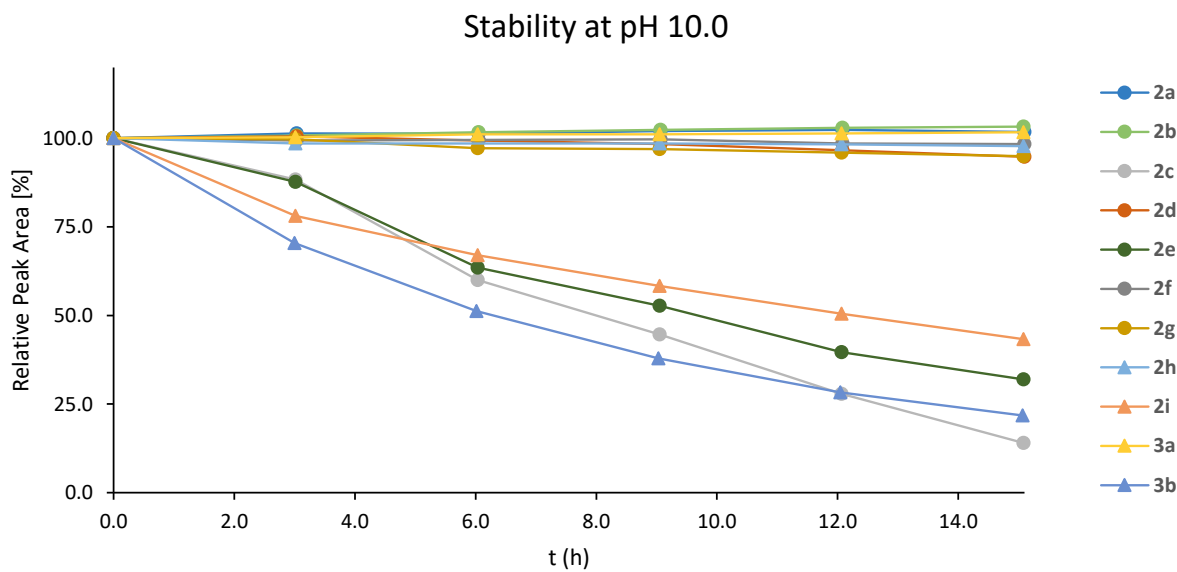


**Figure S16** Stability of complexes (50  $\mu\text{M}$ ) in 1% DMF/phosphate buffer (40 mM, pH 10.0), expressed as relative decrease of the analyte peak area over time in uHPLC runs.

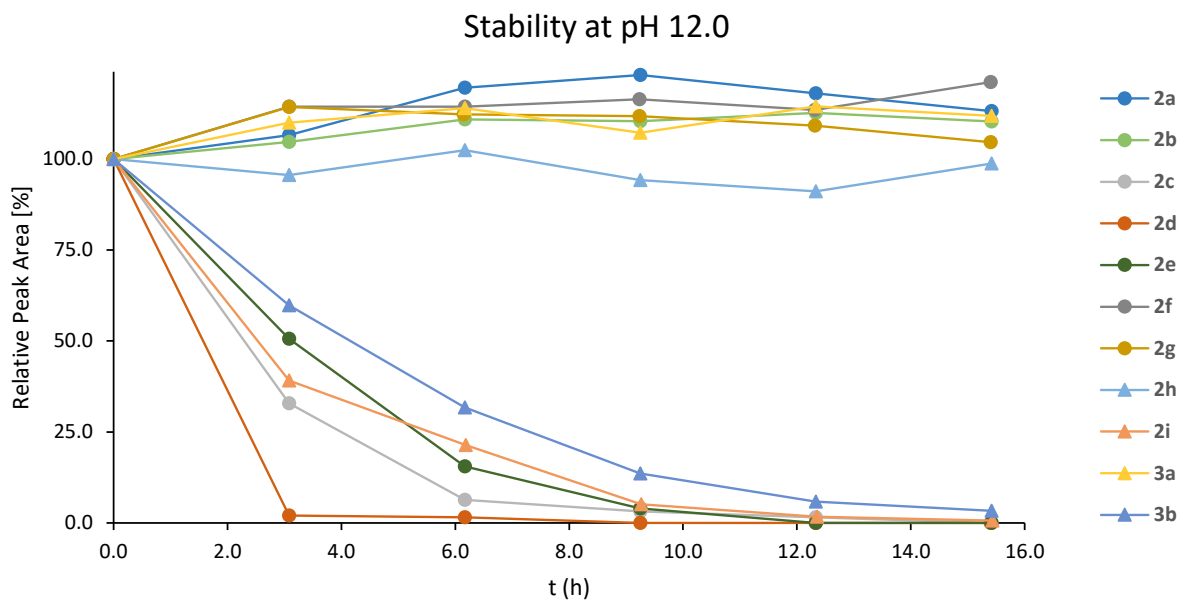


**Figure S17** Stability of complexes ( $50 \mu\text{M}$ ) in 1% DMF/phosphate buffer (40 mM, pH 12.0), expressed as relative decrease of the analyte peak area over time in HPLC runs.

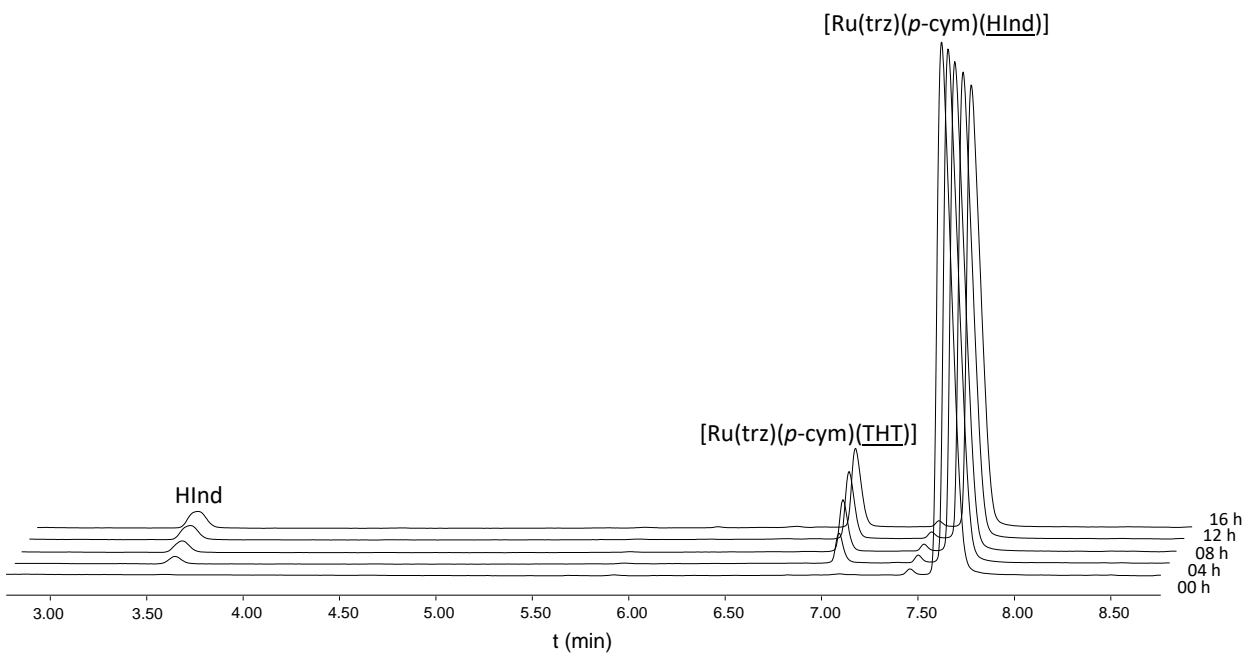


**Figure S18** Overlay of HPLC runs of **2e** ( $50 \mu\text{M}$  in 1% DMF / 40 mM phosphate buffer at pH 3.0) incubated with 10 eq THT collected over 16 h in uHPLC runs.

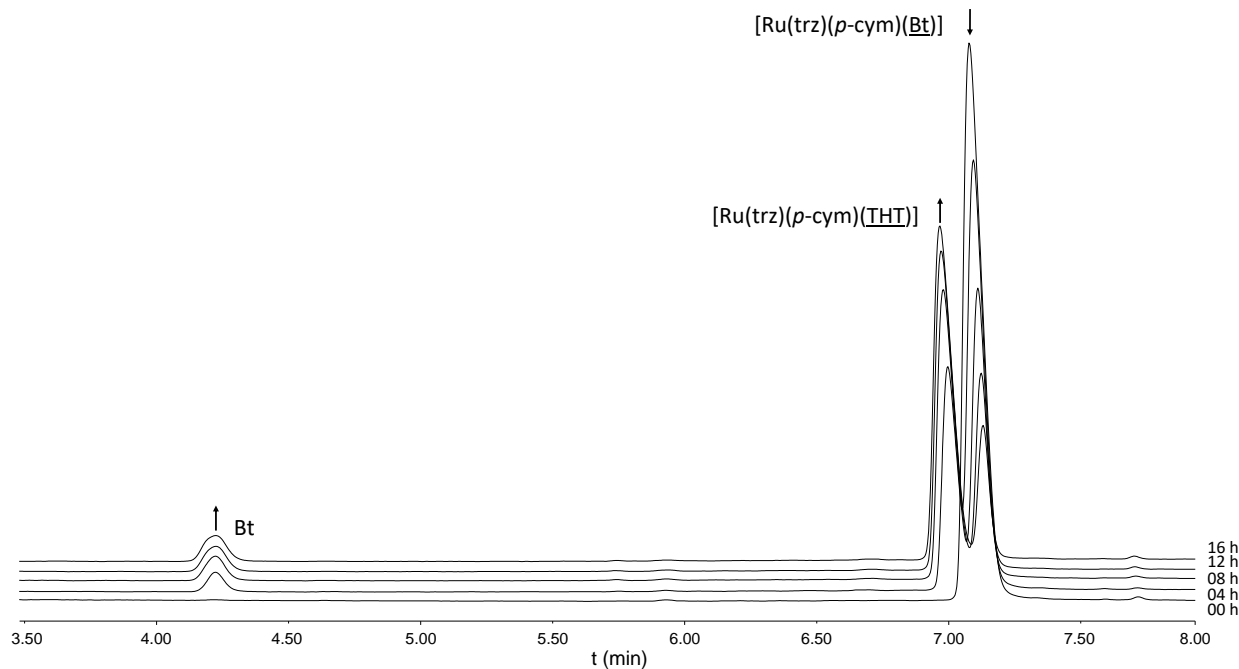


**Figure S19** Overlay of uHPLC runs of **2i** (50  $\mu$ M in 1% DMF / 40 mM phosphate buffer at pH 3.0) incubated with 10 eq THT collected over 16 h.

## 5. Oxidation of **3a**

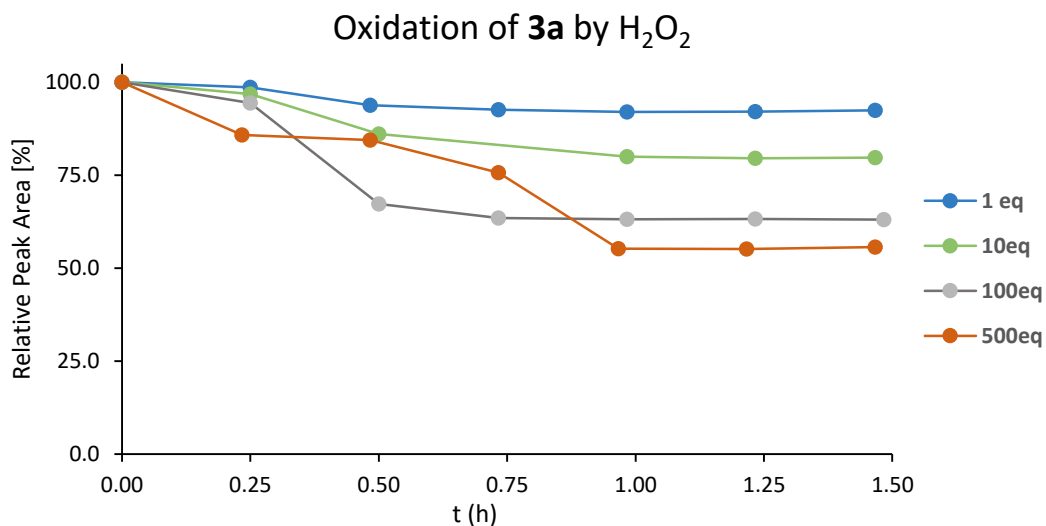


**Figure S20** Oxidation of **3a** (50  $\mu$ M) by hydrogen peroxide in 4 different concentrations to in 1% DMF/phosphate buffer (40 mM, pH 7.4), expressed as relative decrease of the analyte peak area over time in uHPLC runs.

## 6. Amino acid binding studies

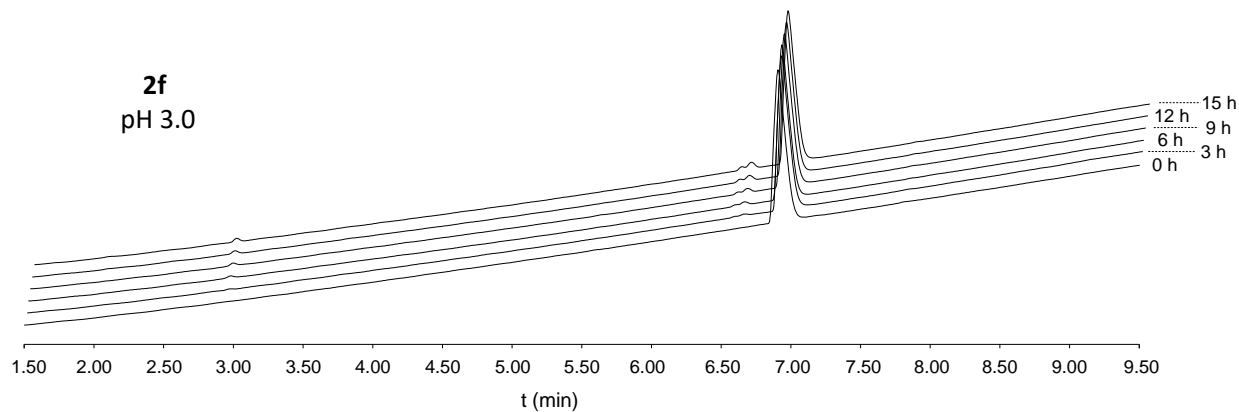


**Figure S21** Overlaid uHPLC chromatograms of **2f** (50  $\mu$ M) incubated with *N*-Ac-His, *N*-Ac-Met, and *N*-Ac-Cys (500  $\mu$ M each) at pH 3.0 collected over 15 h.

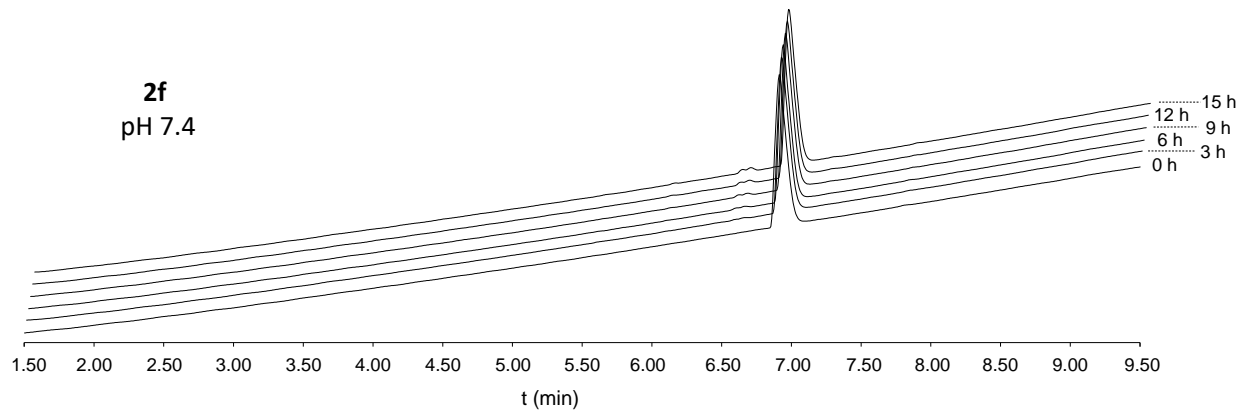


**Figure S22** Overlaid uHPLC chromatograms of **2f** (50  $\mu$ M) incubated with *N*-Ac-His, *N*-Ac-Met, and *N*-Ac-Cys (500  $\mu$ M each) at pH 7.4 collected over 15 h.

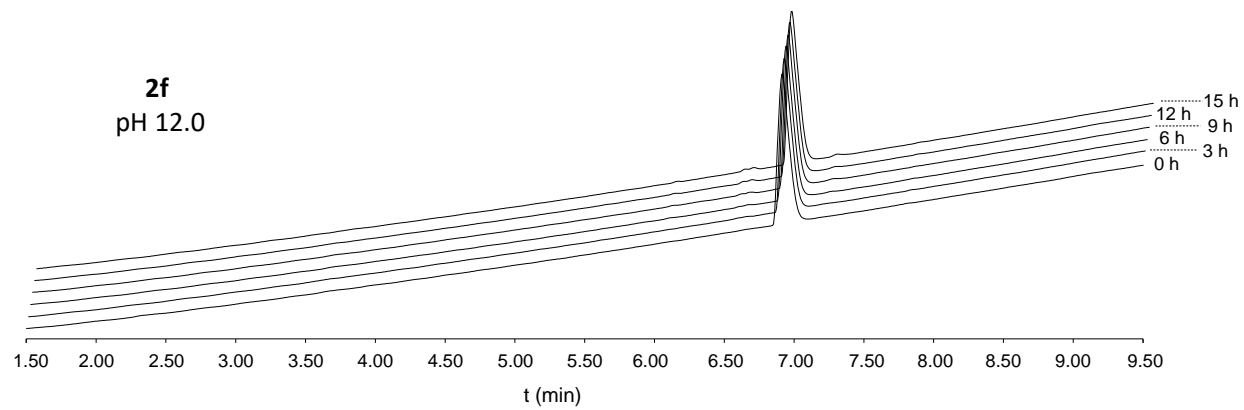


**Figure S23** Overlaid uHPLC chromatograms of **2f** (50  $\mu$ M) incubated with *N*-Ac-His, *N*-Ac-Met, and *N*-Ac-Cys (500  $\mu$ M each) at pH 12.0 collected over 15 h.

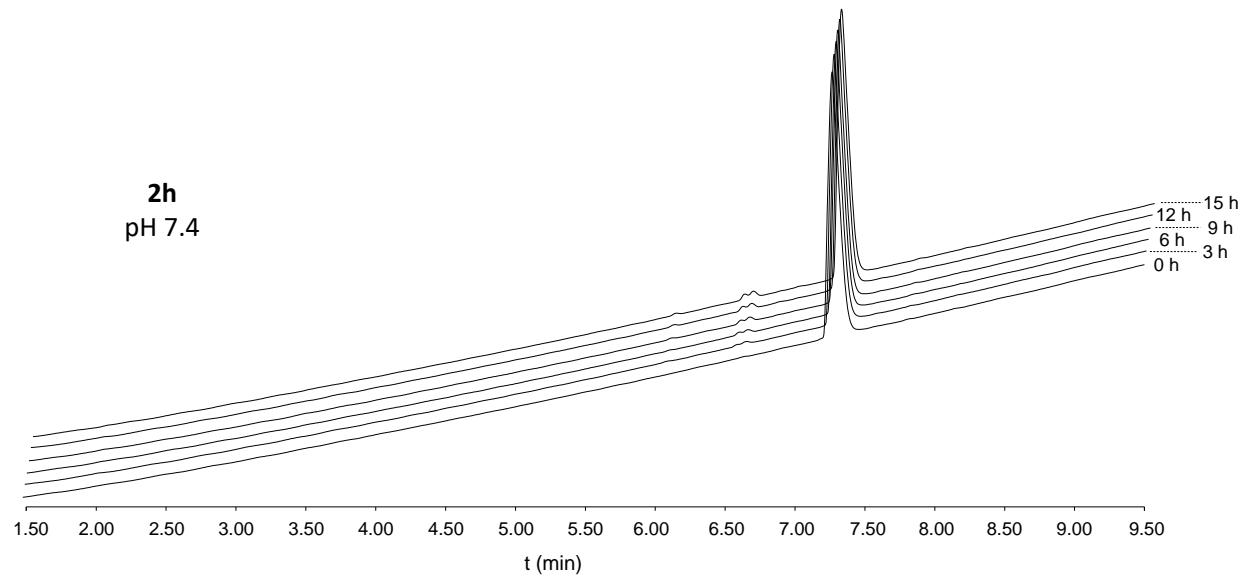


**Figure S24** Overlaid uHPLC chromatograms of **2h** (50  $\mu$ M) incubated with *N*-Ac-His, *N*-Ac-Met, and *N*-Ac-Cys (500  $\mu$ M each) at pH 7.4 collected over 15 h.

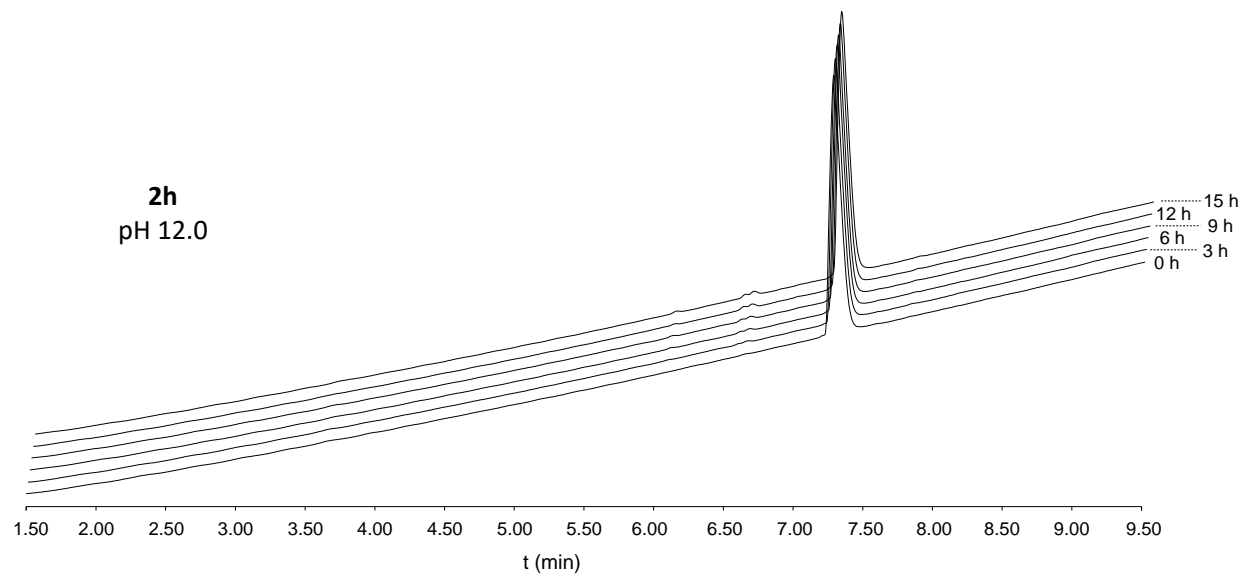


**Figure S25** Overlaid uHPLC chromatograms of **2h** (50  $\mu$ M) incubated with *N*-Ac-His, *N*-Ac-Met, and *N*-Ac-Cys (500  $\mu$ M each) at pH 12.0 collected over 15 h.

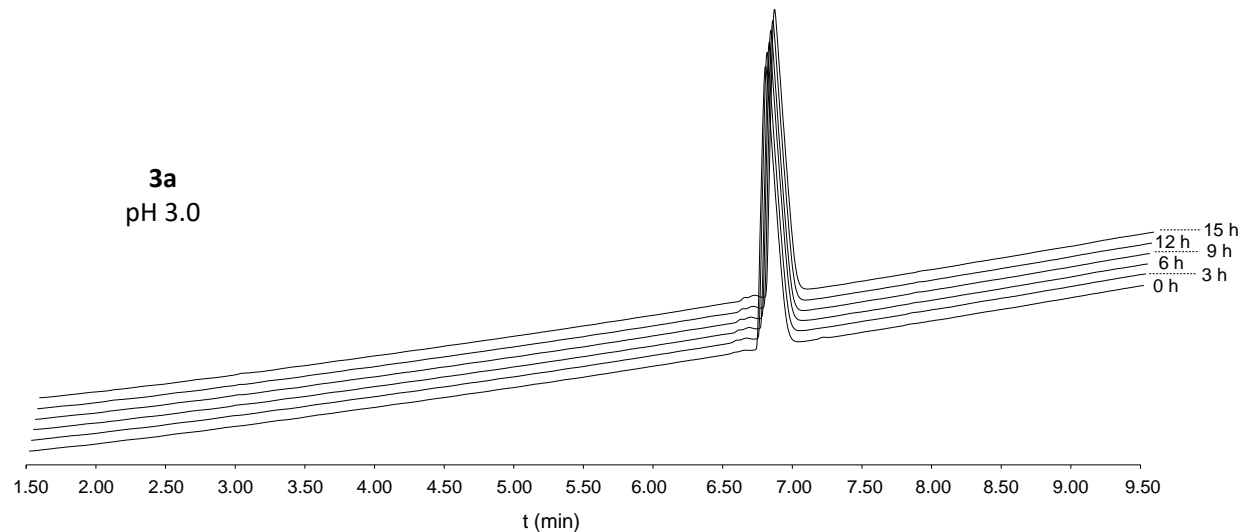


**Figure S26** Overlaid uHPLC chromatograms of **3a** (50  $\mu$ M) incubated with *N*-Ac-His, *N*-Ac-Met, and *N*-Ac-Cys (500  $\mu$ M each) at pH 3.0 collected over 15 h.

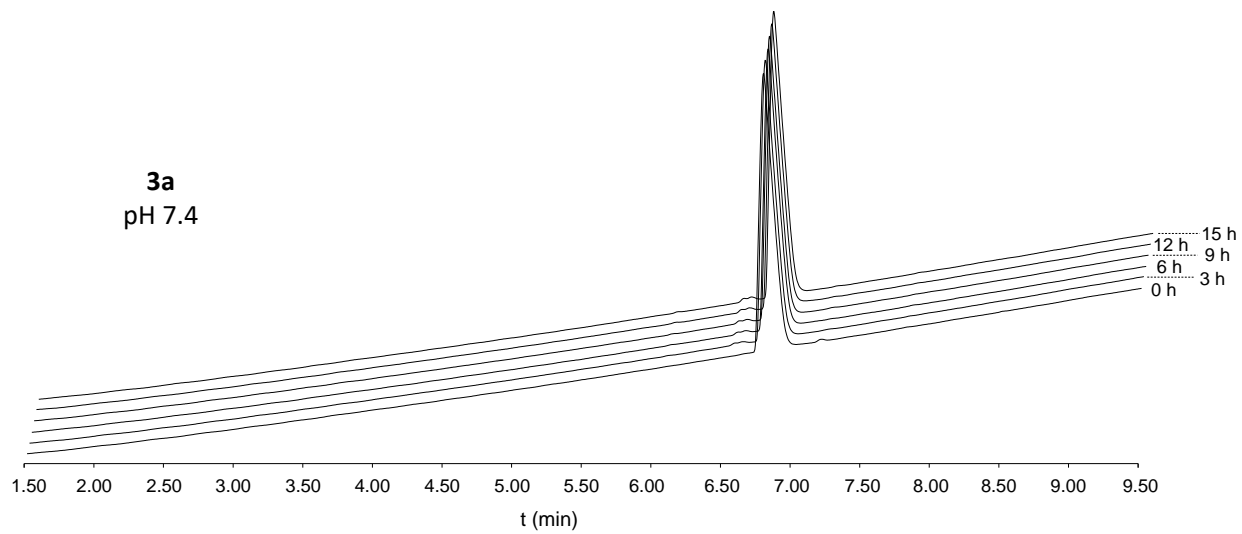


**Figure S27** Overlaid uHPLC chromatograms of **3a** (50  $\mu$ M) incubated with *N*-Ac-His, *N*-Ac-Met, and *N*-Ac-Cys (500  $\mu$ M each) at pH 7.4 collected over 15 h.

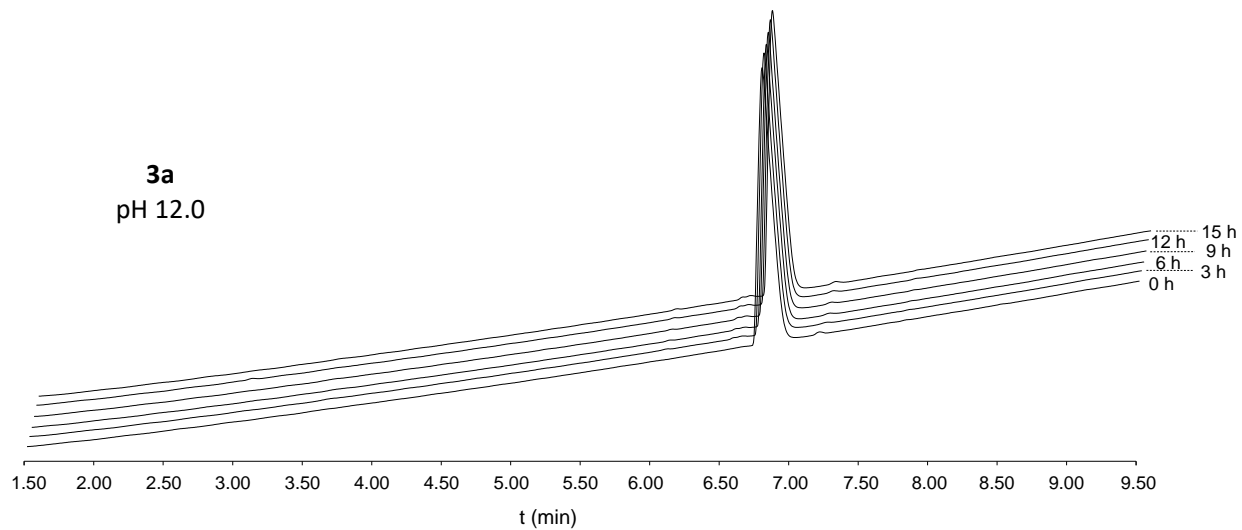


**Figure S28** Overlaid uHPLC chromatograms of **3a** (50  $\mu$ M) incubated with *N*-Ac-His, *N*-Ac-Met, and *N*-Ac-Cys (500  $\mu$ M each) at pH 12.0 collected over 15 h.

7. Chromatographic lipophilicity index  $\varphi_0$

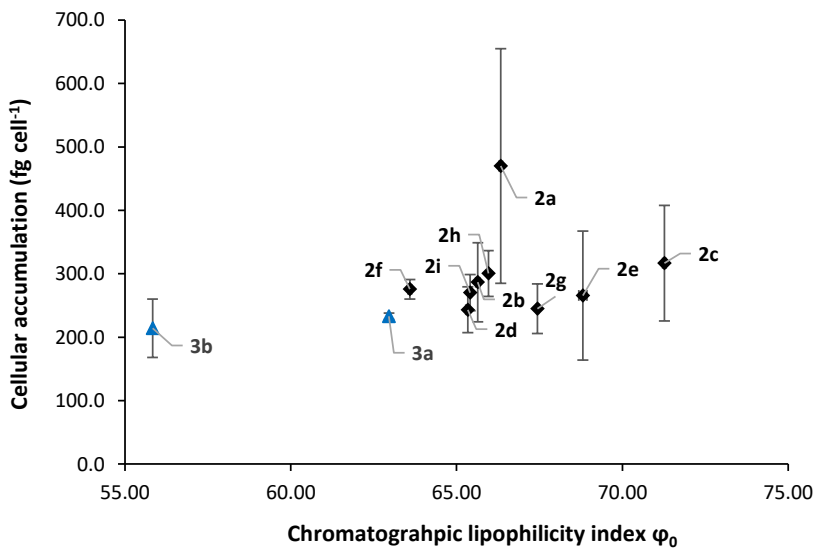


**Figure S29** Scatter plot of chromatographic lipophilicity index  $\varphi_0$  and cellular accumulation in SW480 cells.

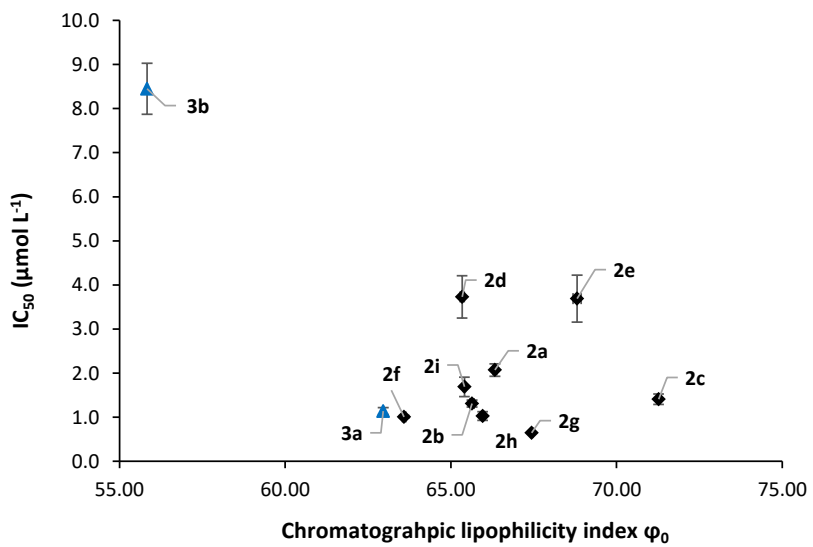


**Figure S30** Scatter plot of chromatographic lipophilicity index  $\varphi_0$  and 50% inhibitory concentration in SW480 cells.

## 8. ROS generation

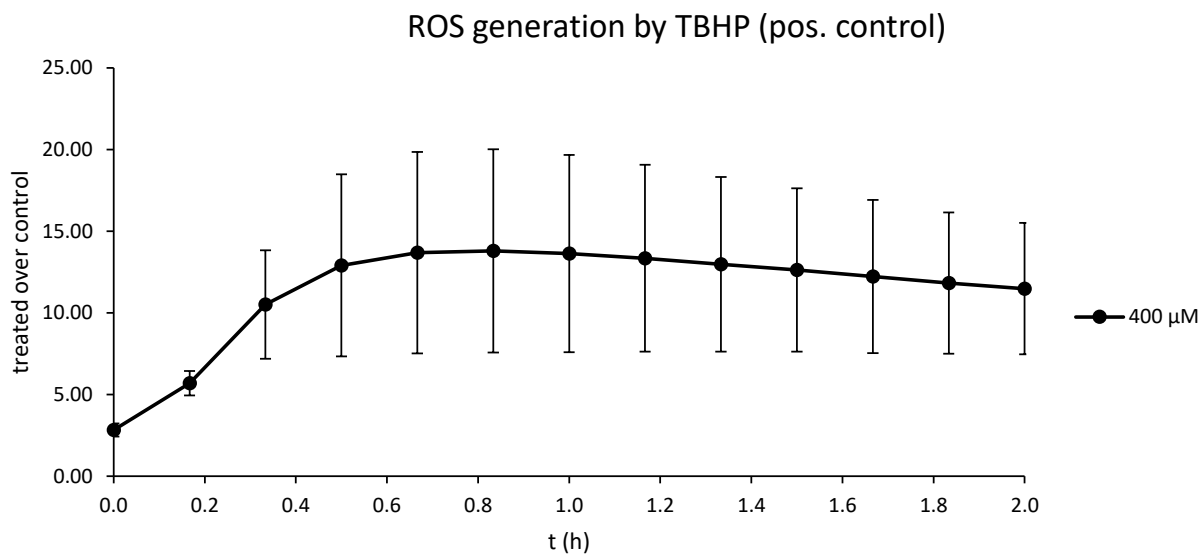


**Figure S31** Level of reactive oxygen species (ROS) upon treatment with *tert*-butyl hydroperoxide at 400  $\mu\text{M}$  over 2 h compared to an untreated control.

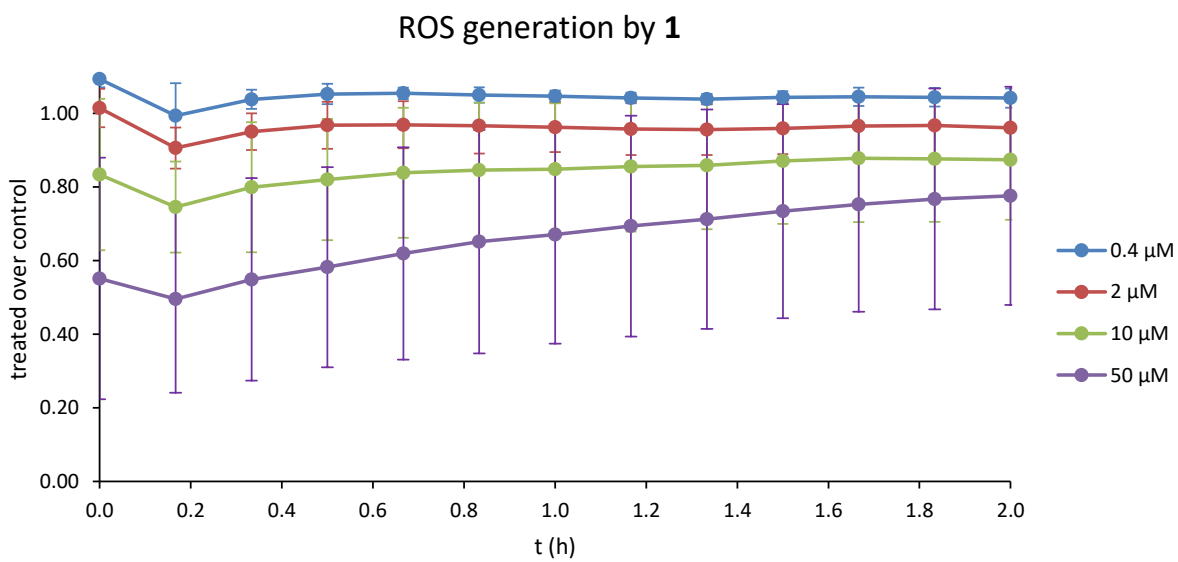


**Figure S32** Level of reactive oxygen species (ROS) upon treatment with **1** at different concentrations over 2 h compared to an untreated control.

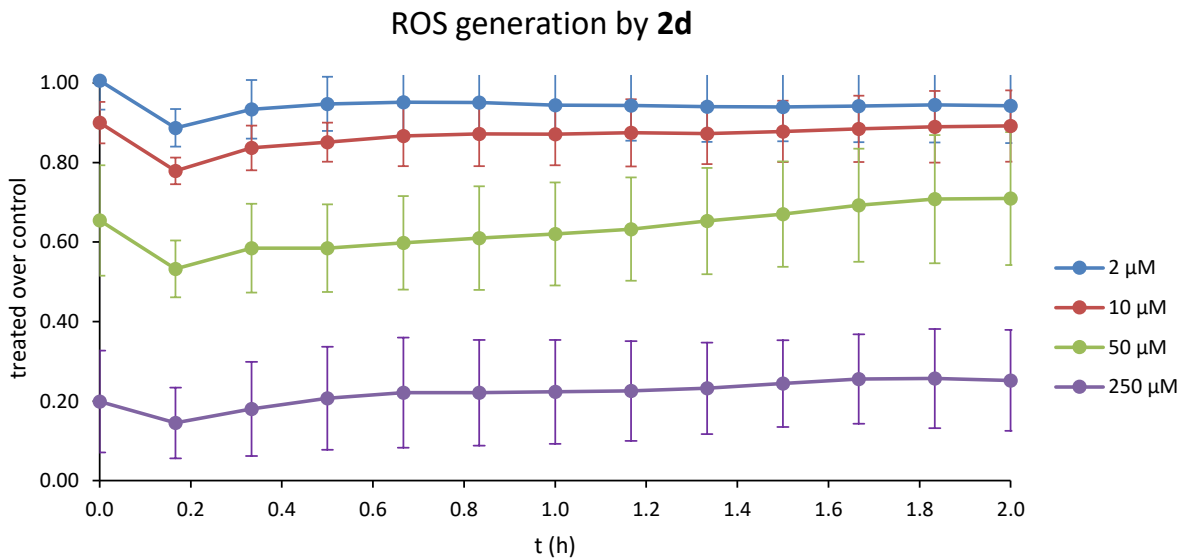


**Figure S33** Level of reactive oxygen species (ROS) upon treatment with **2d** at different concentrations over 2 h compared to an untreated control.

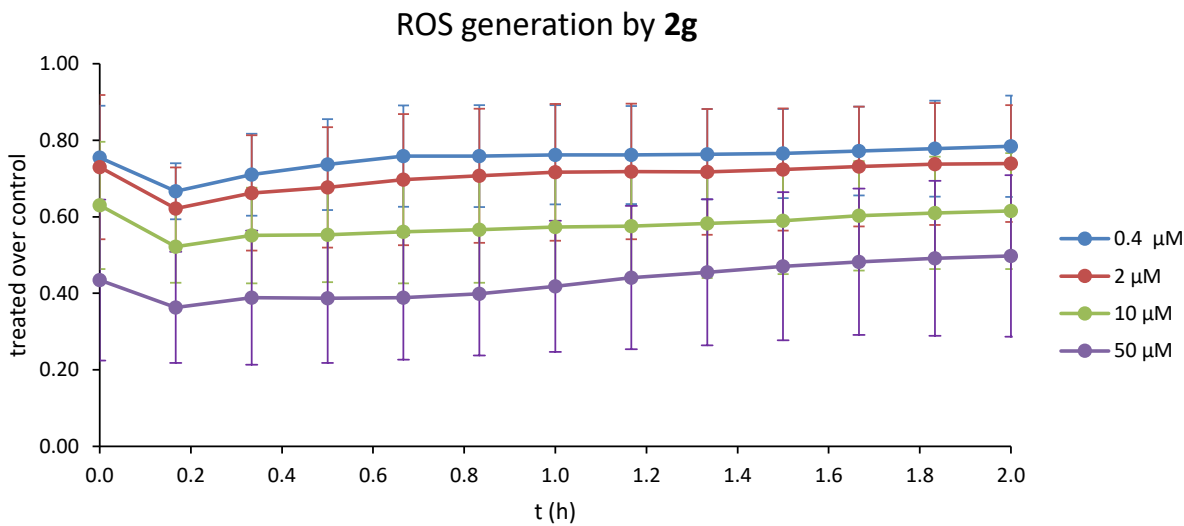


**Figure S34** Level of reactive oxygen species (ROS) upon treatment with **2g** at different concentrations over 2 h compared to an untreated control.

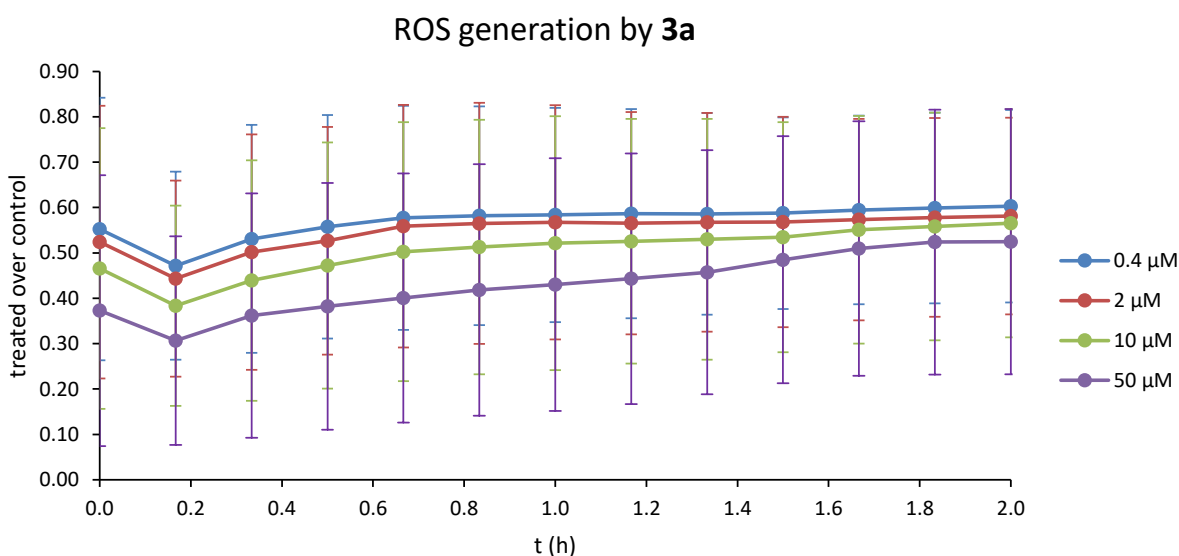


**Figure S35** Level of reactive oxygen species (ROS) upon treatment with **3a** at different concentrations over 2 h compared to an untreated control.

## 9. Methyl green DNA intercalation assay

**Table S13** Percentage of methyl green still bound to preincubated DNA after 24 of incubation with compounds **1**, **2d**, **2g**, and **3a**. Positive control doxorubicin hydrochloride: 65.5% (20 μM), 63.4% (50 μM).

Complex	Methyl green retention			
	0.08 μM	0.4 μM	2 μM	10 μM
<b>1</b>	96.1%	98.5%	99.1%	95.1%
<b>2d</b>	100.0%	99.1%	100.4%	99.9%
<b>2g</b>	98.7%	98.1%	100.1%	99.4%
<b>3a</b>	98.5%	98.8%	100.7%	99.8%

10. Flow cytometric detection of apoptotic cells

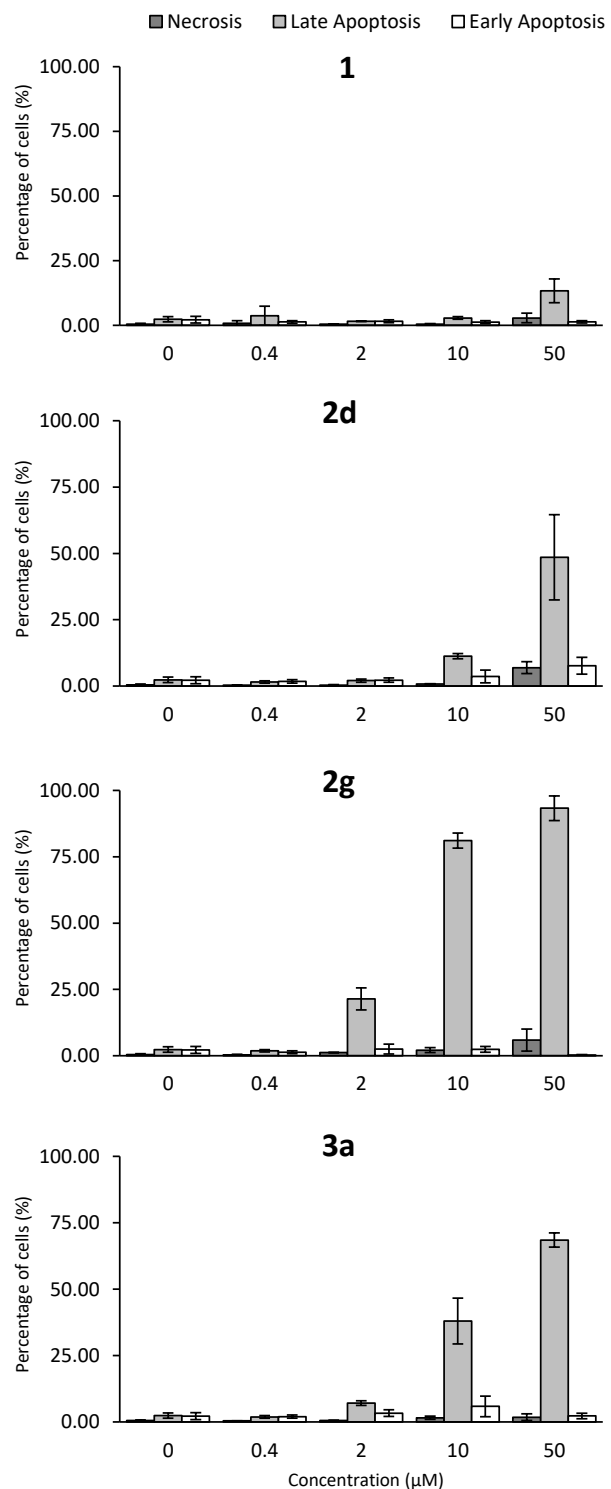


**Figure S36** Induction of apoptosis/necrosis (means  $\pm$  standard deviations) in SW480 24 h after treatment with **1**, **2d**, **2g**, and **3a** at 3 different concentrations and an untreated control.

## 11. $^1\text{H}$ and $^{13}\text{C}$ NMR spectra

### 11.1. [((3- $\kappa\text{N}$ )-1*H*-Imidazole)(1-benzyl-4-(2'- $\kappa\text{C}$ )-phenyl-1,2,3-(3- $\kappa\text{N}$ )-triazolato)( $\eta^6$ -*p*-cymene)ruthenium(II)] nitrate (**2a**)

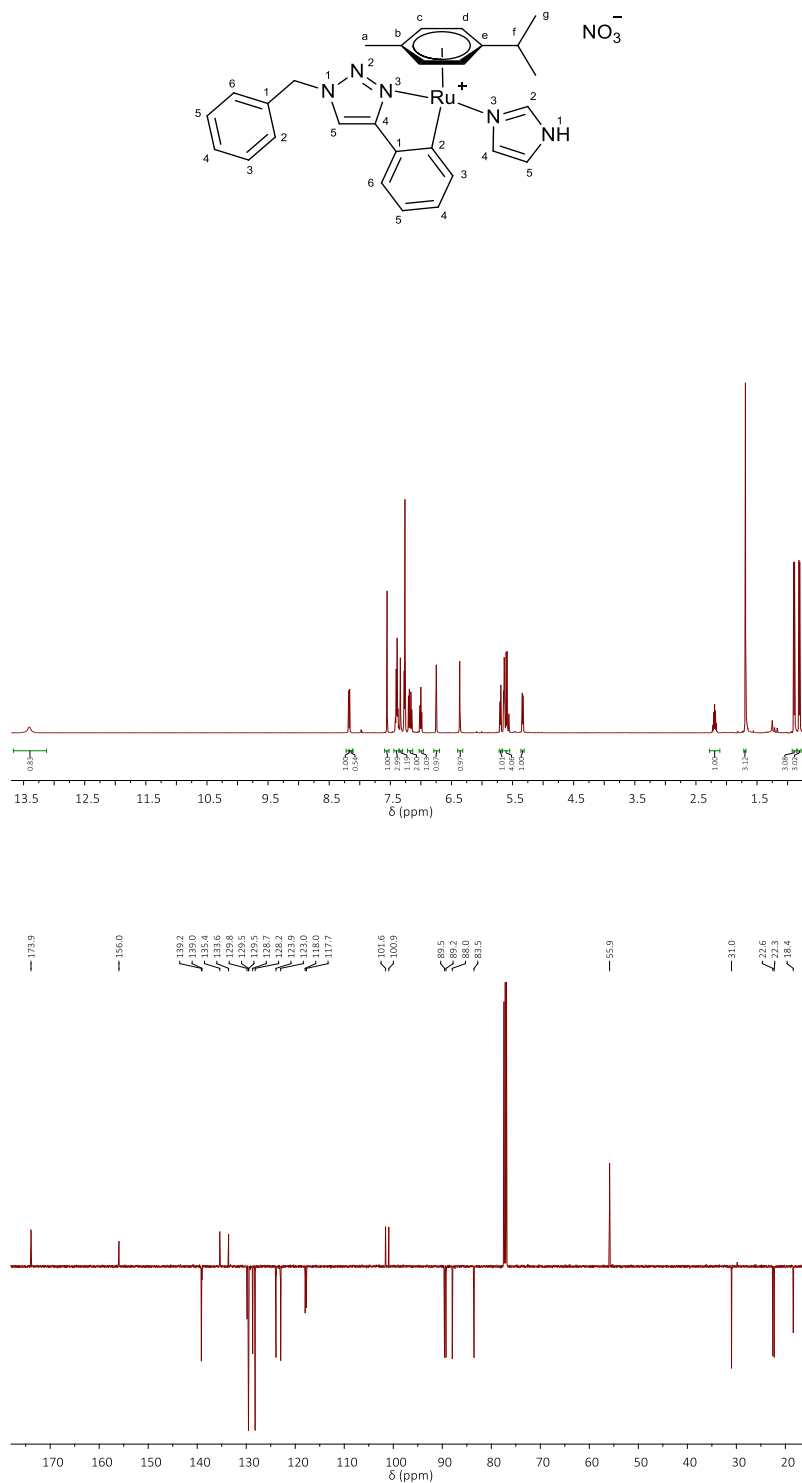


**Figure S37** Numbering scheme (top),  $^1\text{H}$  NMR (middle), and  $^{13}\text{C}$  NMR (bottom) of **2a**.

11.2.  $[(3-\kappa N)\text{-}1\text{-Methylimidazole}(1\text{-benzyl}\text{-}4\text{-(2'-}\kappa C\text{)}\text{-phenyl}\text{-}1,2,3\text{-(3-}\kappa N\text{)}\text{-triazolato})(\eta^6\text{-}p\text{-cymene})\text{ruthenium(II)] nitrate}$  (**2b**)

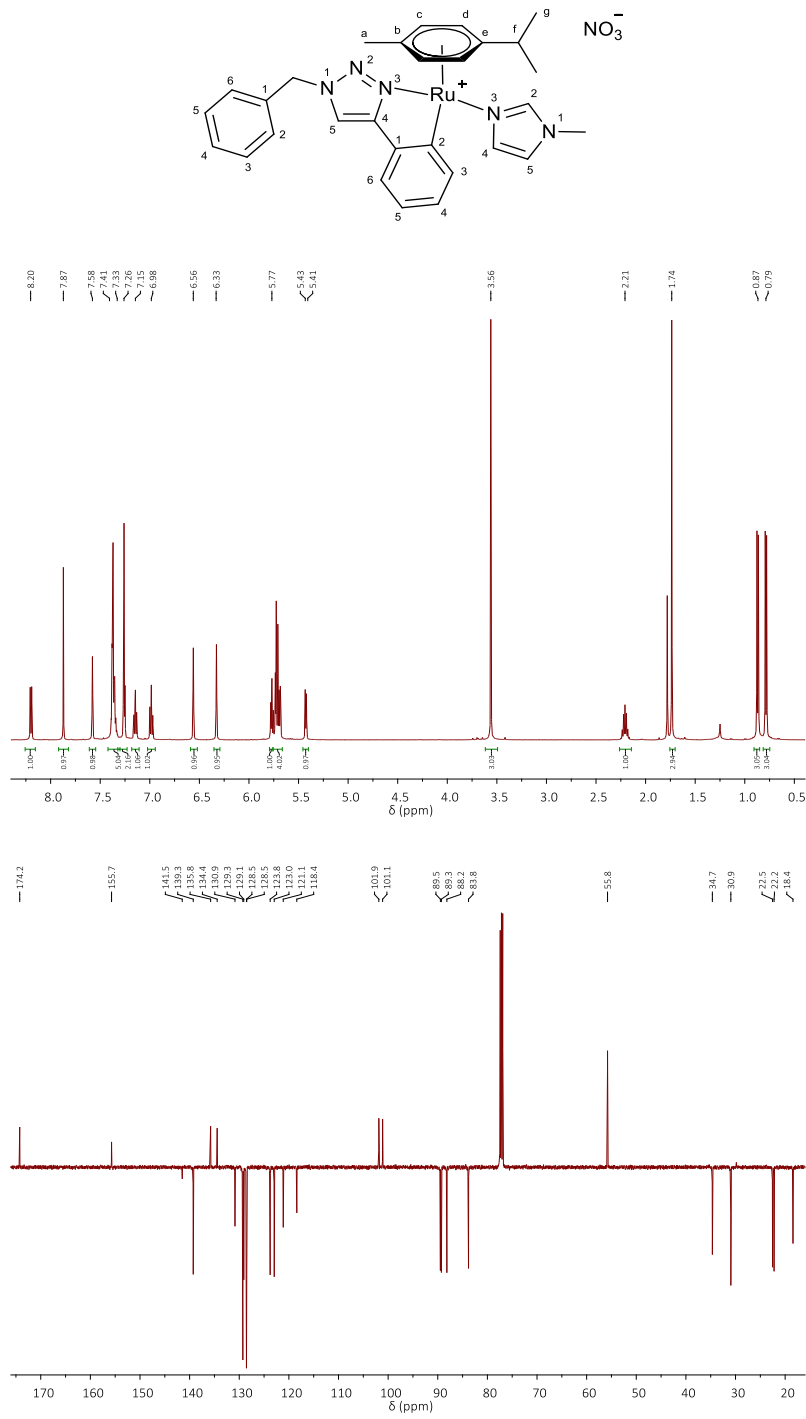


**Figure S38** Numbering scheme (top), <sup>1</sup>H NMR (middle), and <sup>13</sup>C NMR (bottom) of **2b**.

11.3.  $[(3-\kappa N)\text{-}4\text{-Phenylimidazole}(1\text{-benzyl}\text{-}4\text{-(2'-}\kappa C\text{)}\text{-phenyl}\text{-}1,2,3\text{-(3-}\kappa N\text{)}\text{-triazolato})(\eta^6\text{-}p\text{-cymene})\text{ruthenium(II)] nitrate}$  (**2c**)

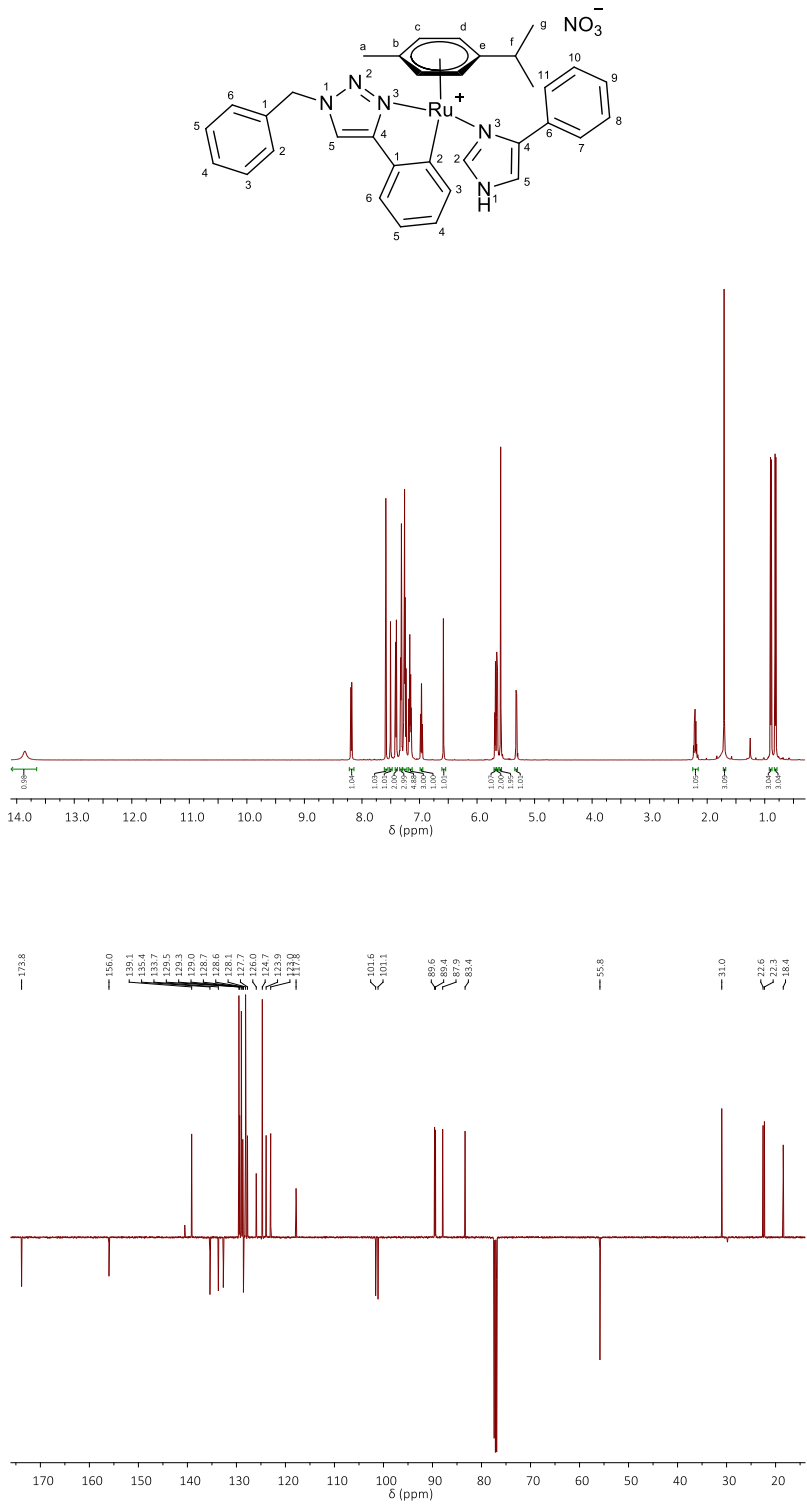


**Figure S39** Numbering scheme (top), <sup>1</sup>H NMR (middle), and <sup>13</sup>C NMR (bottom) of **2c**.

11.4.  $[(2-\kappa N)-1H\text{-Pyrazole})(1\text{-benzyl-}4-(2'\text{-}\kappa C)\text{-phenyl-}1,2,3\text{-(3-}\kappa N\text{)-triazolato})(\eta^6\text{-}p\text{-cymene})\text{ruthenium(II)] nitrate (2d)}$

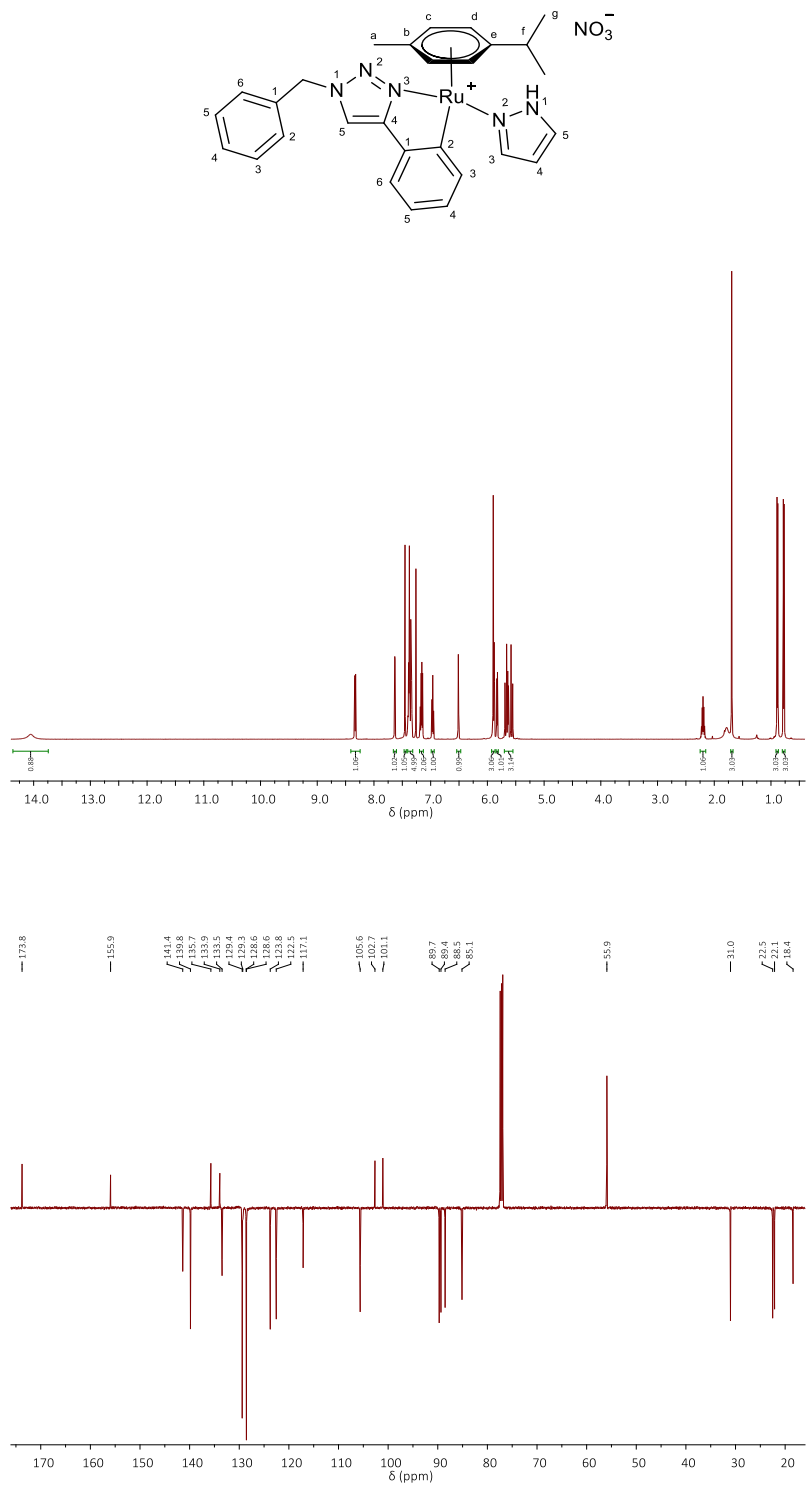


**Figure S40** Numbering scheme (top),  $^1\text{H}$  NMR (middle), and  $^{13}\text{C}$  NMR (bottom) of **2d**.

11.5.  $[(2-\kappa N)-1H\text{-Indazole})(1\text{-benzyl-}4-(2'-\kappa C)\text{-phenyl-}1,2,3-(3-\kappa N)\text{-triazolato})(\eta^6\text{-}p\text{-cymene})\text{ruthenium(II)}]\text{ nitrate}$  (**2e**)

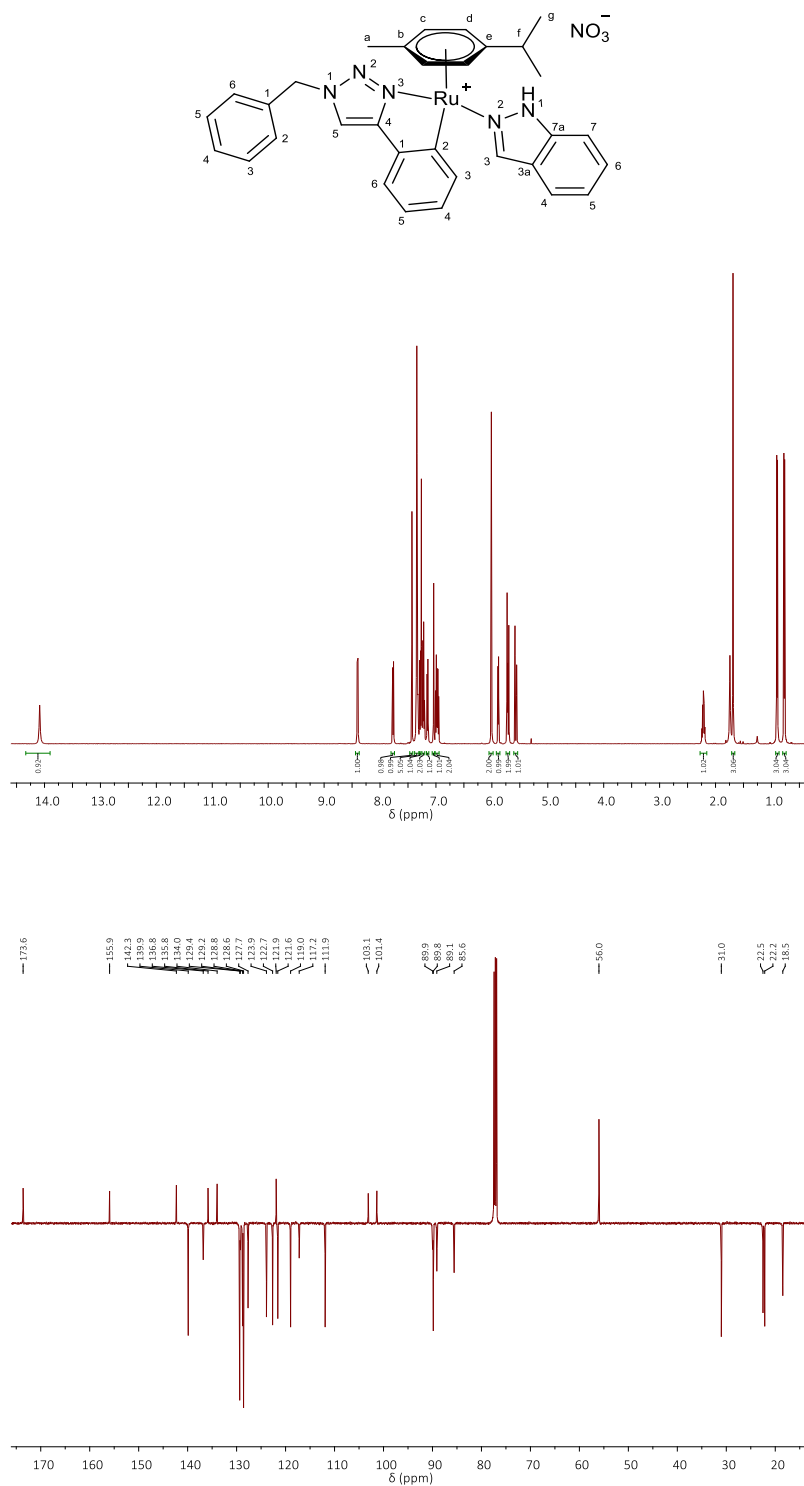


**Figure S41** Numbering scheme (top), <sup>1</sup>H NMR (middle), and <sup>13</sup>C NMR (bottom) of **2e**.

11.6.  $[(\kappa\text{N-Pyridine})(1\text{-benzyl-}4\text{-(2'-}\kappa\text{C)-phenyl-}1,2,3\text{-(3-}\kappa\text{N)-triazolato})(\eta^6\text{-}p\text{-cymene})\text{ruthenium(II)] nitrate (2f)}$

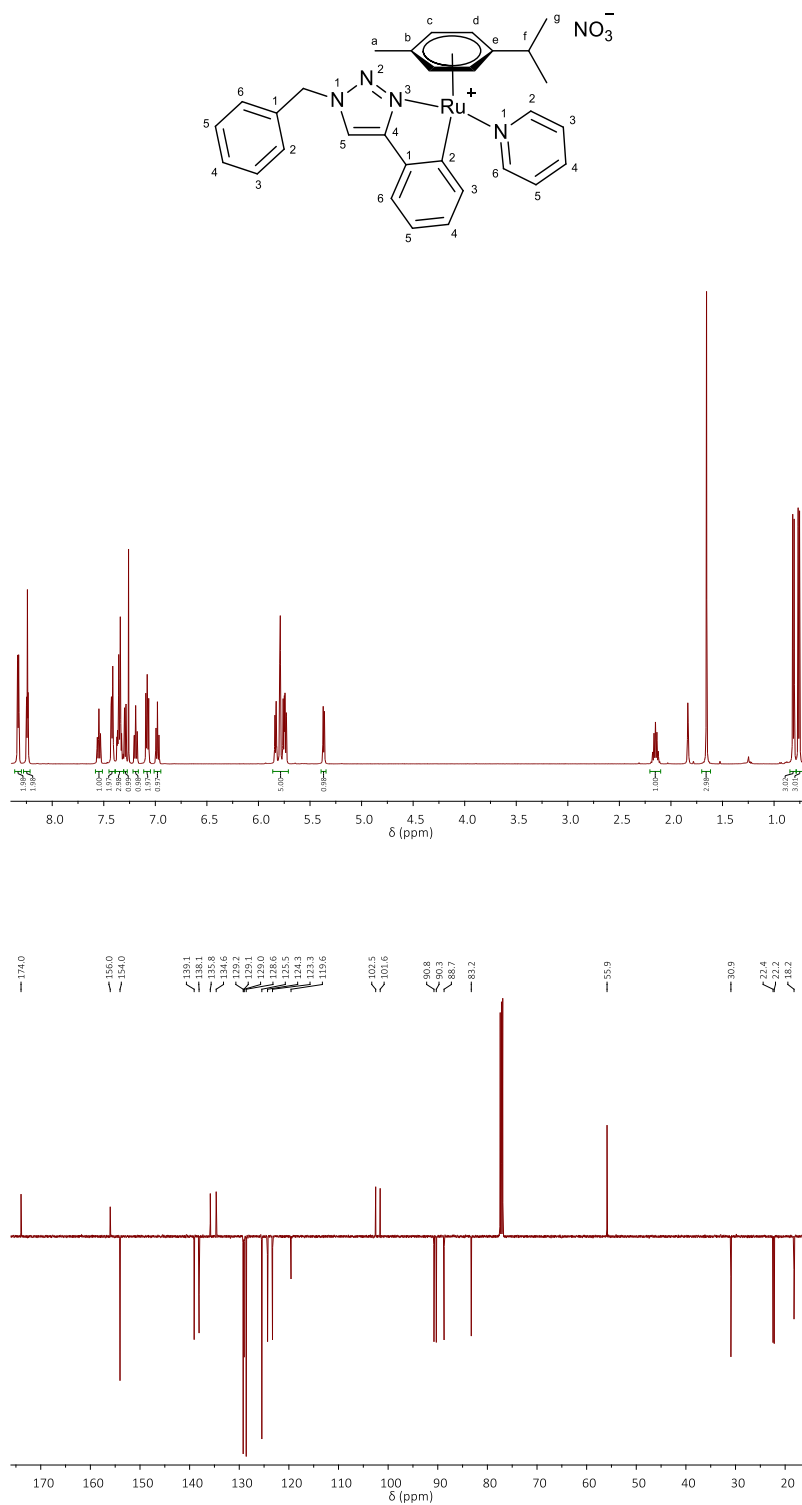


**Figure S42** Numbering scheme (top),  ${}^1\text{H}$  NMR (middle), and  ${}^{13}\text{C}$  NMR (bottom) of **2f**.

11.7. [( $\kappa$ N-Isoquinoline)(1-benzyl-4-(2'- $\kappa$ C)-phenyl-1,2,3-(3- $\kappa$ N)-triazolato)( $\eta^6$ -*p*-cymene)ruthenium(II)] nitrate (**2g**)

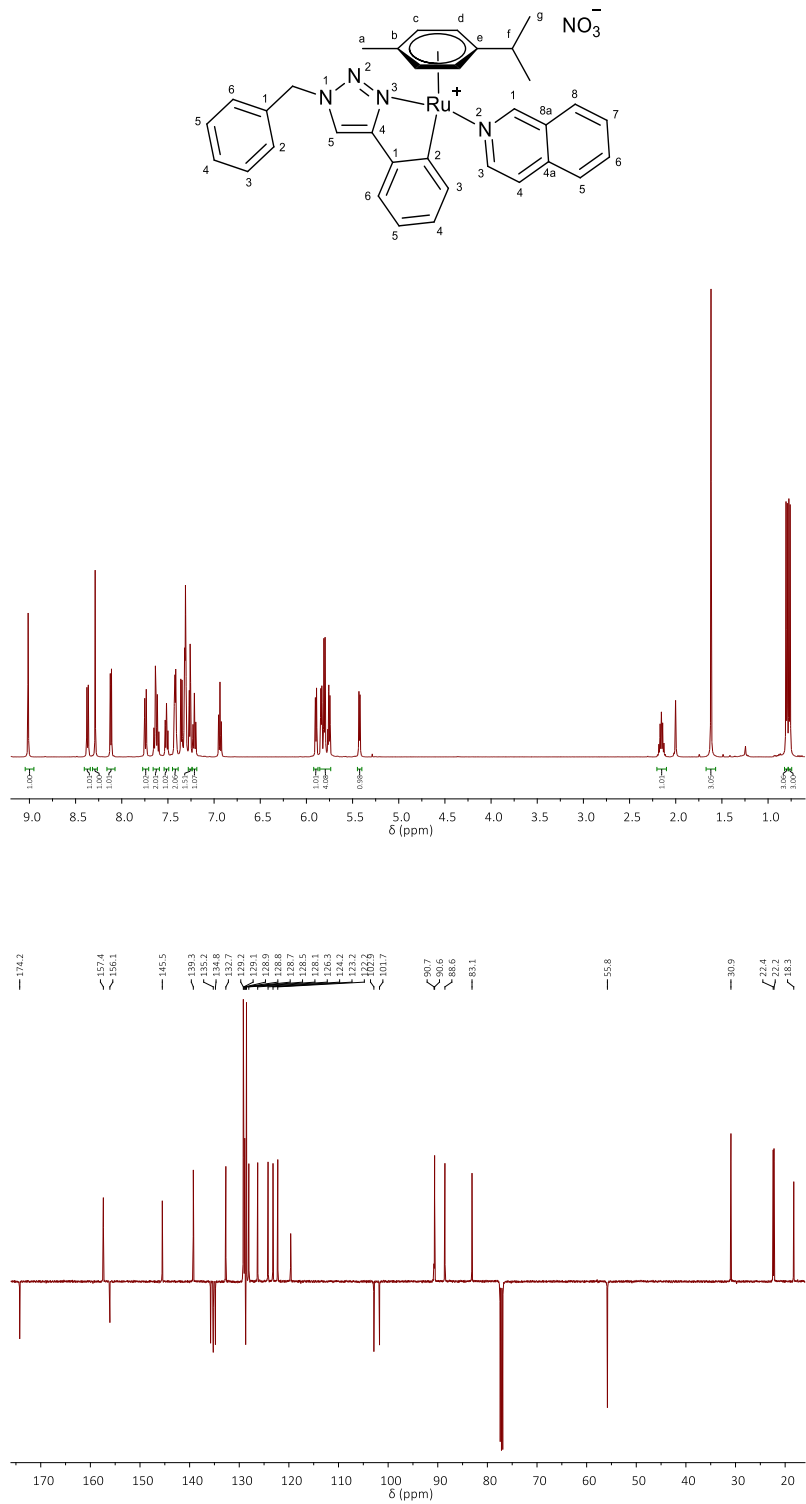


**Figure S43** Numbering scheme (top), <sup>1</sup>H NMR (middle), and <sup>13</sup>C NMR (bottom) of **2g**.

11.8.  $[(1-\kappa N)\text{-Imidazo}[1,2-a]\text{pyridine})(1\text{-benzyl-}4\text{-(2'-}\kappa \text{C)}\text{-phenyl-}1,2,3\text{-(3-}\kappa \text{N)}\text{-triazolato})(\eta^6\text{-}p\text{-cymene})\text{ruthenium(II)] nitrate (2h)}$

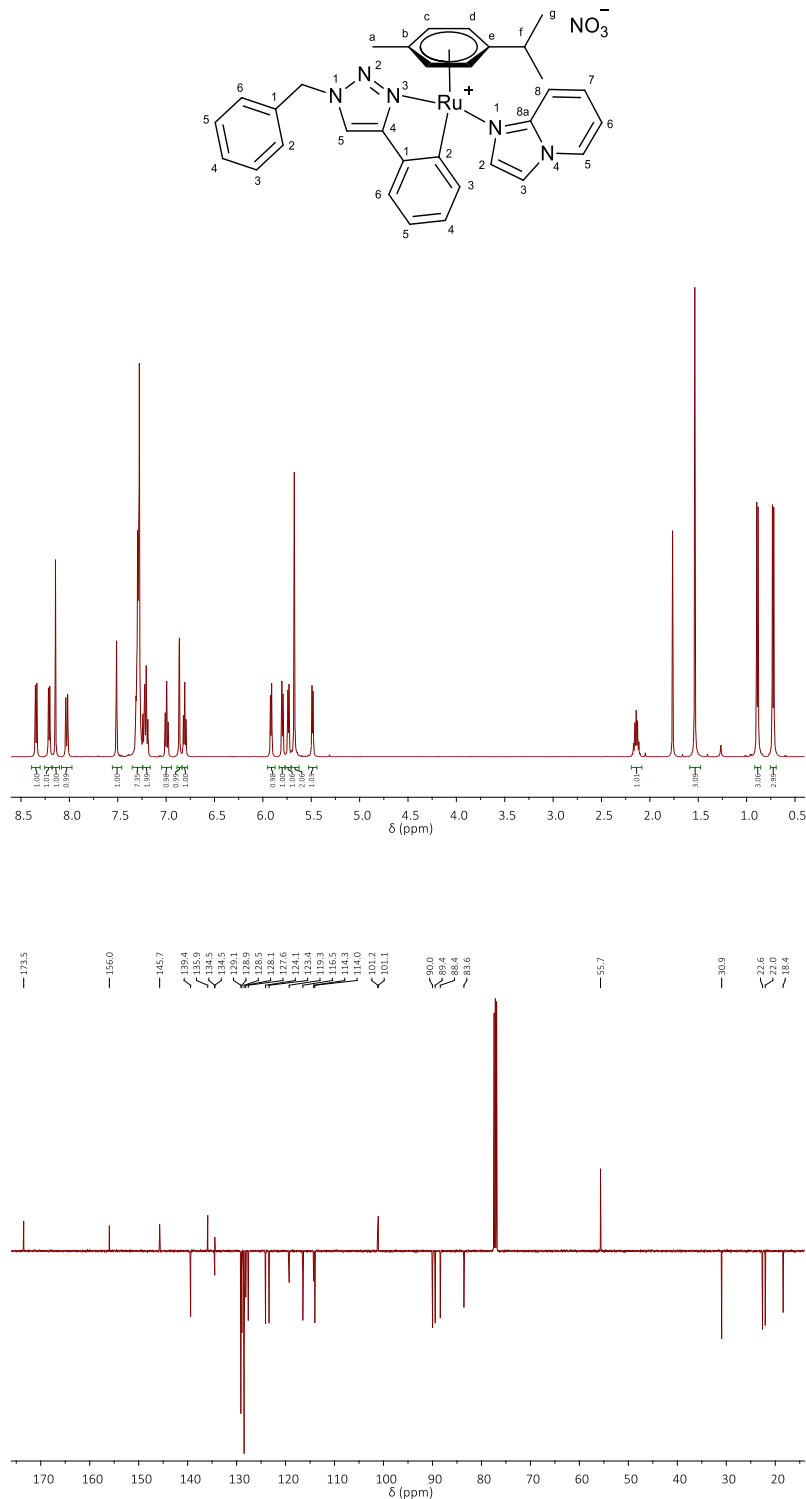


**Figure S44** Numbering scheme (top),  $^1\text{H}$  NMR (middle), and  $^{13}\text{C}$  NMR (bottom) of **2h**.

11.9.  $[(\kappa\text{N}-1,3\text{-Benzothiazol})(1\text{-benzyl-}4\text{-(2'-}\kappa\text{C)-phenyl-}1,2,3\text{-(3-}\kappa\text{N)-triazolato})(\eta^6\text{-}p\text{-cymene})\text{ruthenium(II)}]\text{ nitrate (2i)}$

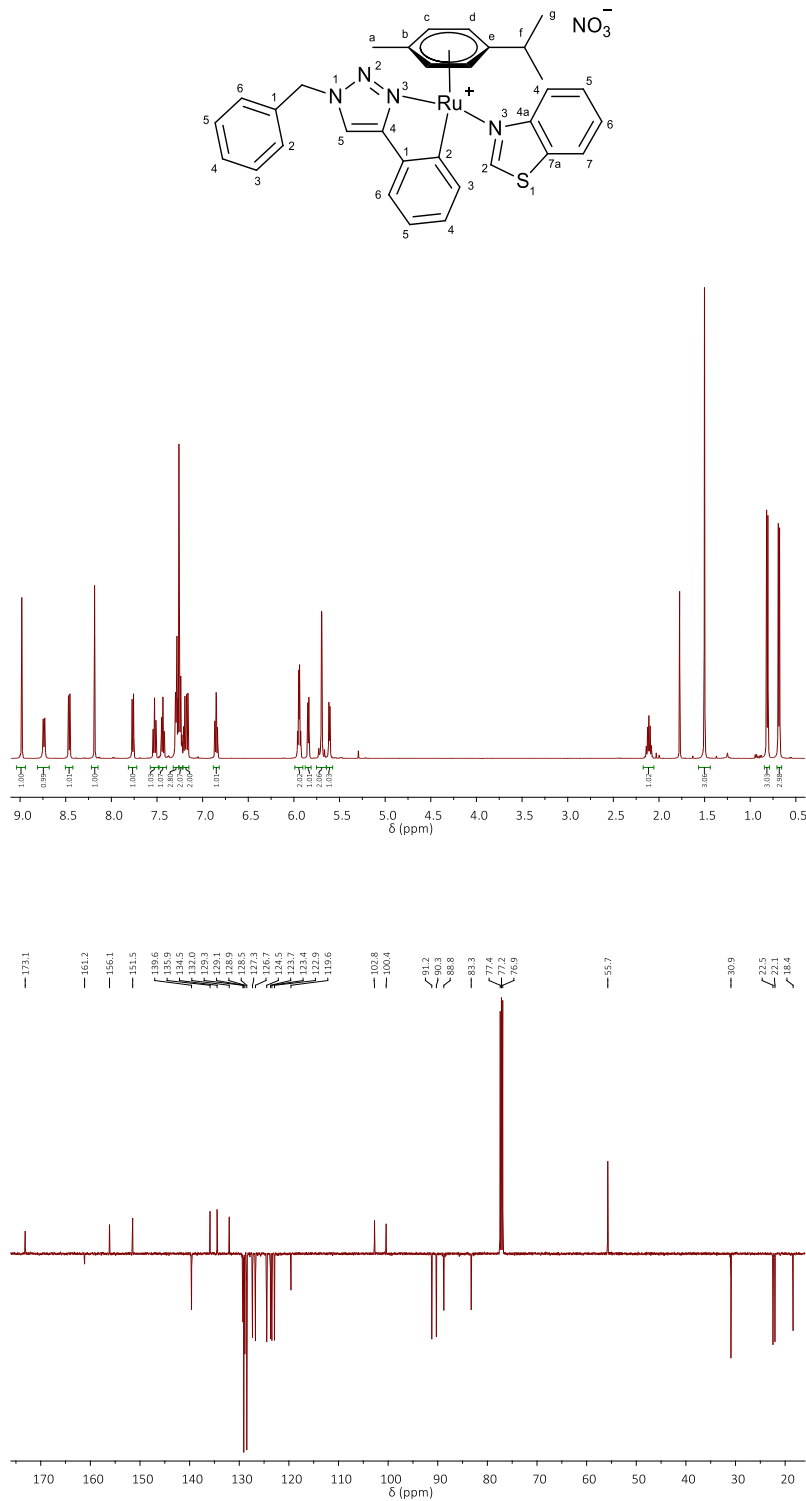


**Figure S45** Numbering scheme (top),  $^1\text{H}$  NMR (middle), and  $^{13}\text{C}$  NMR (bottom) of **2i**.

11.10. [( $\kappa$ S-(Methylsulfanyl)methan)(1-benzyl-4-(2'- $\kappa$ C)-phenyl-1,2,3-(3- $\kappa$ N)-triazolato)( $\eta^6$ -*p*-cymene)ruthenium(II)] nitrate (**3a**)

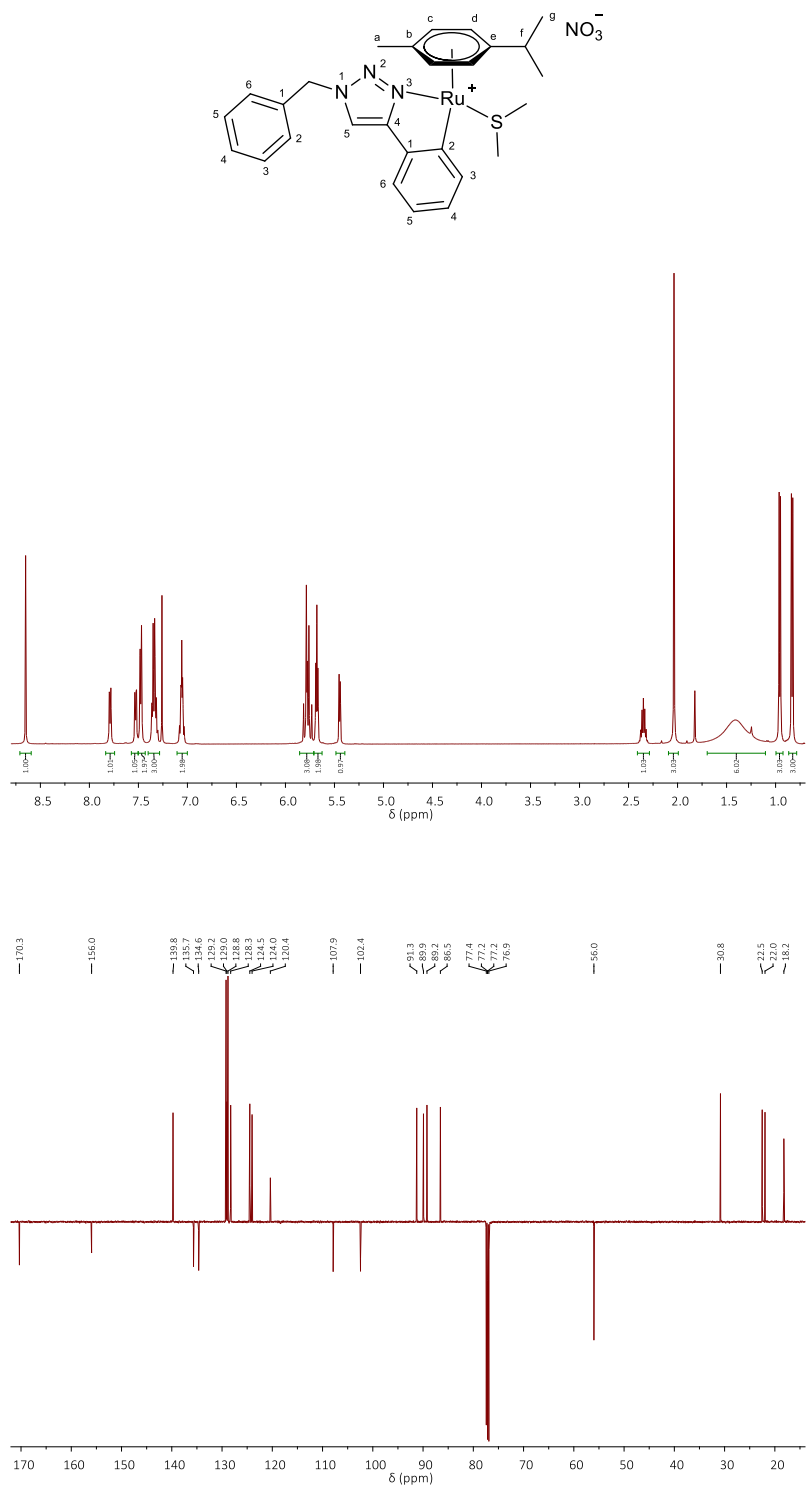


**Figure S46** Numbering scheme (top), <sup>1</sup>H NMR (middle), and <sup>13</sup>C NMR (bottom) of **3a**.

11.11. [( $\kappa$ S-Dimethyl sulfoxide)(1-benzyl-4-(2'- $\kappa$ C)-phenyl-1,2,3-(3- $\kappa$ N)-triazolato)( $\eta^6$ -*p*-cymene)ruthenium(II)] nitrate (**3b**)

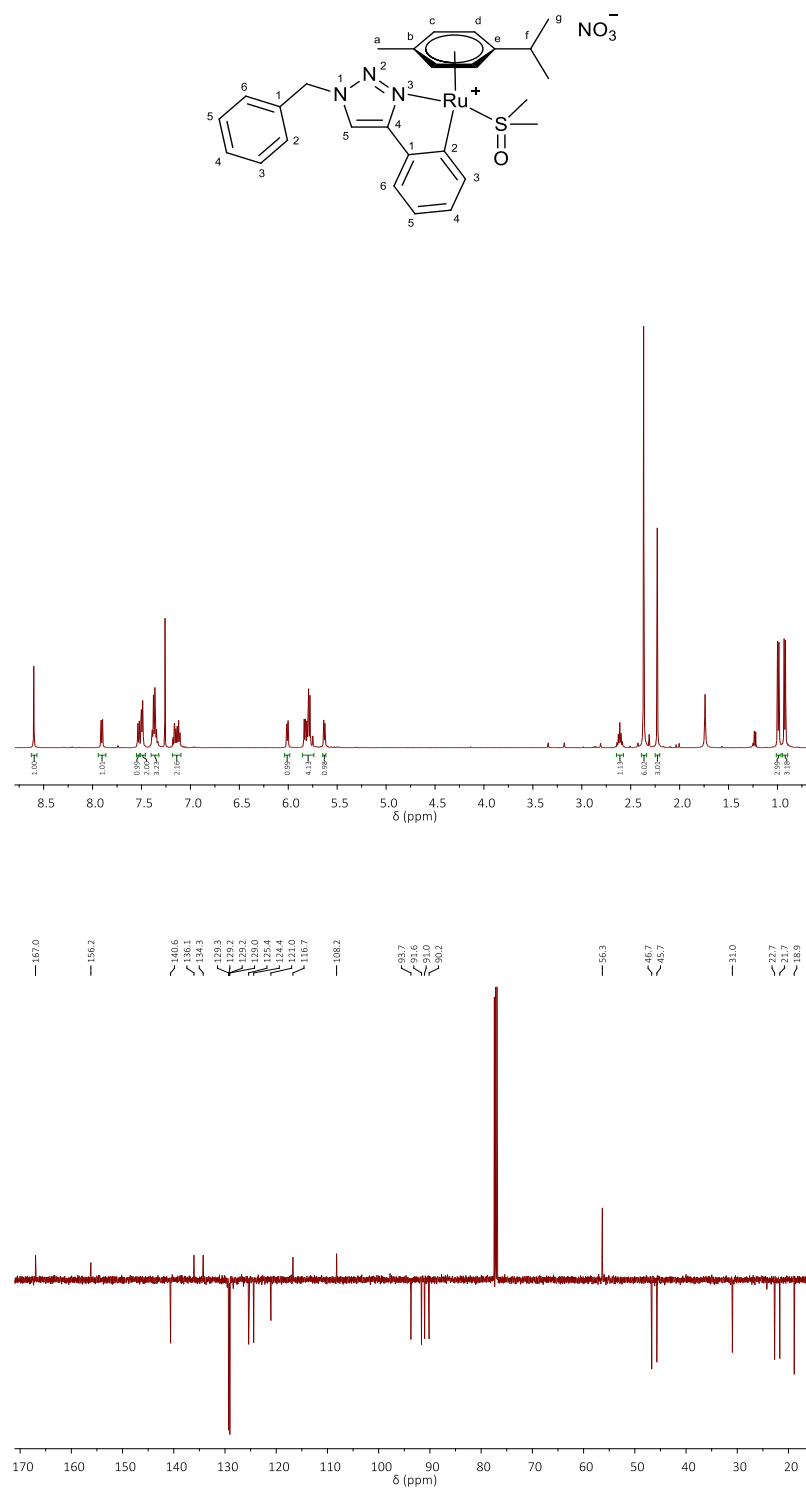


**Figure S47** Numbering scheme (top), <sup>1</sup>H NMR (middle), and <sup>13</sup>C NMR (bottom) of **3b**.